construction engineering research laboratory

TECHNICAL REPORT E-91
May 1976
Solar Energy for Heating and Cooling of Buildings

INTERIM FEASIBILITY ASSESSMENT METHOD FOR SOLAR HEATING AND COOLING OF ARMY BUILDINGS

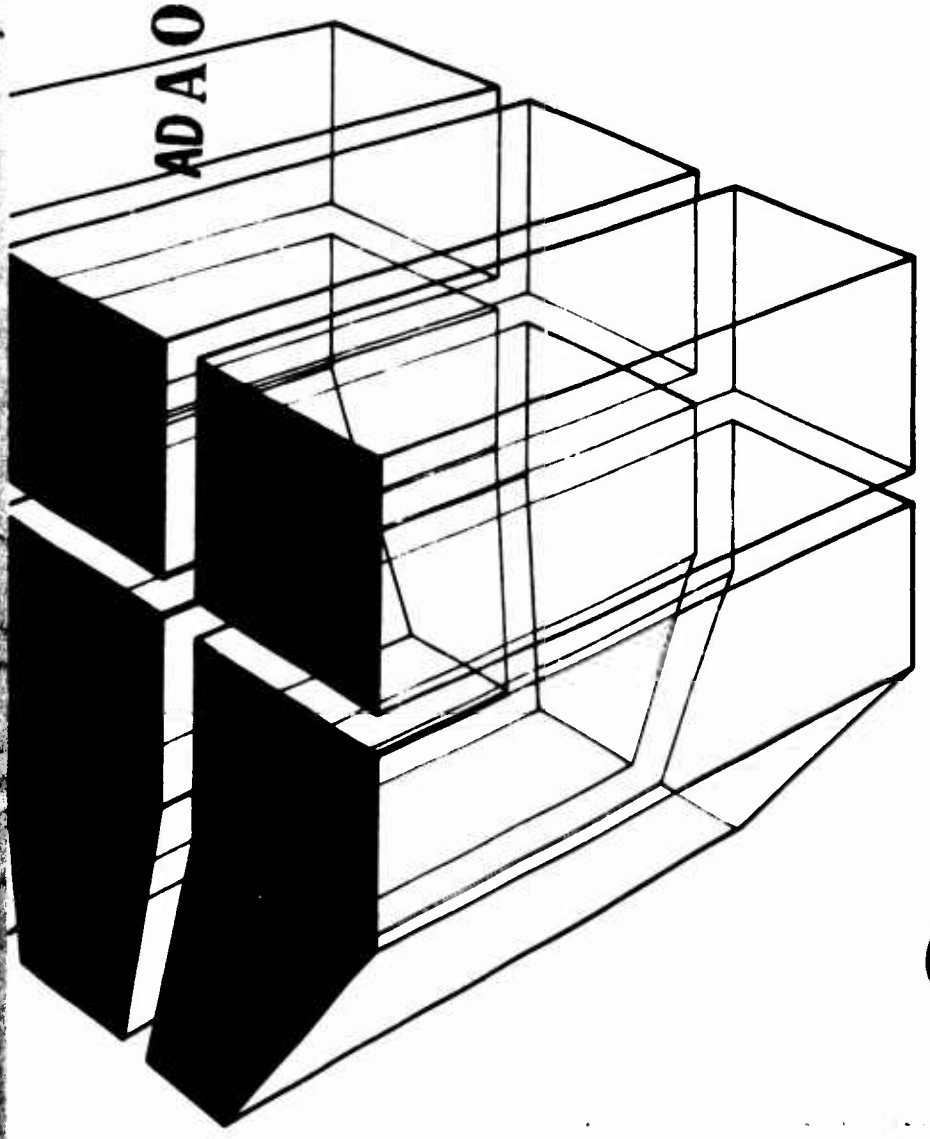

by
D. Hittle
D. Holshouser
G. Walton

CERL

UNCLASSIFIED

SECURITY CLASSIFICATION OF THIS PAGE (When Data Entered)

REPORT DOCUMENTATION PAGE	READ INSTRUCTIONS BEFORE COMPLETING FORM
1. REPORT NUMBER: TECHNICAL REPORT E-91	2. GOVT ACCESSION NO. / 3. RECIPIENT'S CATALOG NUMBER
4. TITLE (and Subtitle): INTERIM FEASIBILITY ASSESSMENT METHOD FOR SOLAR HEATING AND COOLING OF ARMY BUILDINGS.	5. TYPE OF REPORT & PERIOD COVERED: FINAL rept.
	6. PERFORMING ORG. REPORT NUMBER
7. AUTHOR(s): Doug [redacted] Hittle, D. Holshouser, G. Walton	8. CONTRACT OR GRANT NUMBER(s)
9. PERFORMING ORGANIZATION NAME AND ADDRESS: CONSTRUCTION ENGINEERING RESEARCH LABORATORY, P.O. Box 4005, Champaign, Illinois 61820	10. PROGRAM ELEMENT, PROJECT, TASK AREA & WORK UNIT NUMBERS: ~~A~~763734DT08-06-001
11. CONTROLLING OFFICE NAME AND ADDRESS	12. REPORT DATE: May 1976
	13. NUMBER OF PAGES: 49
14. MONITORING AGENCY NAME & ADDRESS (if different from Controlling Office): CERL-TR-E-91	15. SECURITY CLASS. (of this report): UNCLASSIFIED
	15a. DECLASSIFICATION/DOWNGRADING SCHEDULE
16. DISTRIBUTION STATEMENT (of this Report): Approved for public release; distribution unlimited. 51p.	
17. DISTRIBUTION STATEMENT (of the abstract entered in Block 20, if different from Report): RDT/E-4-A-763734-DT-08 OR	
18. SUPPLEMENTARY NOTES: Copies are obtainable from National Technical Information Service, Springfield, VA 22151 RDT/E-4-A-763734-DT-0806	
19. KEY WORDS (Continue on reverse side if necessary and identify by block number): solar heating and cooling; solar energy; computer simulations	

20. ABSTRACT (Continue on reverse side if necessary and identify by block number)

This report discusses design considerations for heating and cooling buildings with solar energy. General criteria are provided for selecting the components and configuration of such a system. The report presents parametric computer simulation studies for two buildings of typical construction at five locations in the United States. Hourly building heating and cooling loads were computed for each building at each site using the National Bureau of Standards Load Determining Program (NBSLD) and hourly weather data. Using these loads, hourly simulation studies were performed to determine the effects of collector

OVER

DD FORM 1 JAN 73 1473 EDITION OF 1 NOV 65 IS OBSOLETE

UNCLASSIFIED 405279

SECURITY CLASSIFICATION OF THIS PAGE (When Data Entered)

AB

type, collector area, collector tilt angle, thermal energy storage tank volume, and heat exchanger effectiveness on simulated solar heating and cooling system performance.

The results of more than 200 one-year solar system simulations are presented. In addition, a dimensionless graph and methodology are provided which can be used to estimate solar heating and cooling system performance for buildings and sites other than those studied. The report provides an explanation and an example of an approach for determining the life cycle cost of a solar-equipped building as compared to a conventional installation. Descriptions of the NBSLD program and the solar heating and cooling simulation program are provided.

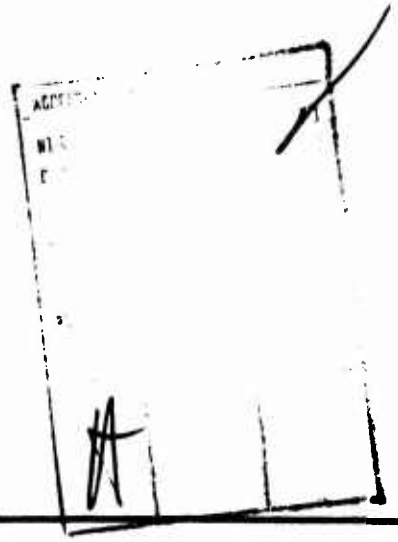

FOREWORD

This study was performed by the U. S. Army Construction Engineering Research Laboratory (CERL) under RDT&E Project 4A763734DT08, "Military Construction Engineering Development," Task 06, "Energy Conservation," Work Unit 001, "Solar Energy for Heating and Cooling of Buildings." The applicable Requirement Code is QCR 1.05.008. Work was performed under the technical direction of the Office of the Chief of Engineers (OCE), Directorate of Military Construction. Mr. S. Hiratsuka was the OCE Technical Monitor.

Mr. D. Hittle of CERL's Energy Branch (EPE), Energy and Power Division (EP) was Principal Investigator for this project. Dr. D. Leverenz is Chief of EPE, and Mr. R. Donaghy is Chief of EP.

COL. M. D. Remus is Commander and Director of CERL, and Dr. L. R. Shaffer is Deputy Director.

CONTENTS

FIGURES

TABLES

INTERIM FEASIBILITY ASSESSMENT METHOD FOR SOLAR HEATING AND COOLING OF ARMY BUILDINGS

1 INTRODUCTION

Background

Like all energy users, the Army is faced with a rapidly increasing energy bill and, in some locations, a shortage or curtailment of its energy supply. Therefore, the Army must look for new natural energy sources, especially those which are abundant and are not subject to inflation. The most ideal source is solar energy, because of its abundance, widespread distribution, and absence of recurring fuel cost. Therefore, solar energy systems offer tremendous potential as alternate energy sources for heating and cooling Army installations, if technically feasible utilization systems can be developed which are economically competitive with conventional fuels.

The technical feasibility of heating and cooling buildings using flat-plate solar collectors has been established both in theory and practice. Although future demonstrations, including the Army's plans for a solar demonstration at Fort Hood, TX, will indicate improvements in component design and manufacturing and in system design methods, investigators can approach solar heating and cooling technology with full confidence that a practical, reliable system can be constructed. Although the design phase may be somewhat more complex, the construction phase requires little more skill than is required to install conventional heating and cooling systems. The decision whether to apply solar energy for heating and cooling should therefore generally be based on life cycle cost comparisons, taking into consideration the escalating price and decreasing availability of conventional fuels.

Purpose

The purpose of this report is to provide a method to perform a preliminary economic feasibility assessment of candidate solar heating and cooling systems when applied to specific buildings at specific sites.

Approach

The economic assessment of solar energy systems involves comparing conventional life-cycle fuel costs with the additional first cost of installing a solar energy system and the resulting reduced operating costs. The principal problem of this analysis is determining the amount of energy that the solar energy system can economically supply to meet the heating and cooling requirements of specific buildings and sites. Unfortunately, simple design calculations generally do not provide a basis for determining either the annual building energy requirements or the fraction of those requirements that can be met economically with solar energy. Computer simulation techniques must usually be used for these design calculations.

To develop the feasibility assessment techniques, computer simulation was used to perform detailed analysis of numerous candidate solar heating and cooling systems for test case buildings at various sites. Based on analysis results, a general-purpose, dimensionless curve was developed which can be directly applied to other buildings and sites to estimate expected performances of candidate solar heating and cooling systems. Using this estimated performance, a simplified method was developed to initially assess the potential economic viability of the solar project without expending considerable funds and effort for detailed analysis.

Scope

Only heating and cooling applications using solar energy were considered, so assessment results do not apply when only solar heating is being considered. Combined solar heating and cooling was the exclusive consideration primarily because the annual energy requirement for cooling heavily dominated that of heating for the buildings and sites studied. This dominance can be expected as long as current comfort cooling design trends are applied. Performance curves for solar heating only are presently being developed, and these will be the subject of a separate report.

Chapter 2 of this report briefly describes solar heating and cooling systems and their components. Chapter 3 presents the simulation studies results and the curves and equations necessary to estimate expected solar heating and cooling system performance for buildings and sites not studied. Chapter 4 presents a graphical method for determining the lowest life-cycle cost solar heating and cooling system and for determining its economic viability. Chapter 5 presents the report's conclusions and recommendations.

Appendix A provides an example application of the economic feasibility assessment methods described in Chapter 4. Appendix B describes the National

Bureau of Standards Load Determining Program (NBSLD) application to the barracks and battalion headquarters and classroom buildings. Appendix C is a detailed description of the solar heating and cooling simulation model.

2 COMPONENTS OF A SOLAR INSTALLATION

Generalized System

Figure 1 is a schematic diagram of a basic system for heating and cooling with solar energy. In comparison to conventional systems, the only unique features are the collector array and the thermal energy storage tank.

The sunlight falling on the array warms a fluid (usually glycol and water), which is pumped through the solar collectors. The heat from this fluid is transferred within a heat exchanger to a second fluid (usually water), which is pumped to an insulated thermal storage tank. When there is a heating or cooling demand, the warm fluid from the storage tank is either pumped directly to the heat exchanger in the duct or to the cooling unit. In most feasible systems, the temperature in the tank will occasionally drop below useful values; it is, therefore, necessary to include in the system an auxiliary heater capable of supplying all or part of the heating or cooling demand.

Solar Collectors

The function of a solar collector is to capture as much available sunlight as possible and to convert this energy to heat energy. Converting solar energy to heat at low and moderate temperatures (80°F to 300°F [24.6°C to 148.7°C]) involves components which are in low-volume, commercial production. This temperature range is adequate for heating and cooling buildings and will be considered in this report.

Two types of solar energy fall on a collector: that coming directly from the sun (beam energy) and that coming from other directions through scattering or reflection of the sun's rays (diffuse energy). On a clear day, the intensity of diffuse energy is much less than that of beam energy, but the former is often intense enough to be useful during cloudy or smoggy conditions.

Tracking and Concentrating Collectors

To maximize the amount of beam energy collected, the solar collectors can be continually moved so that

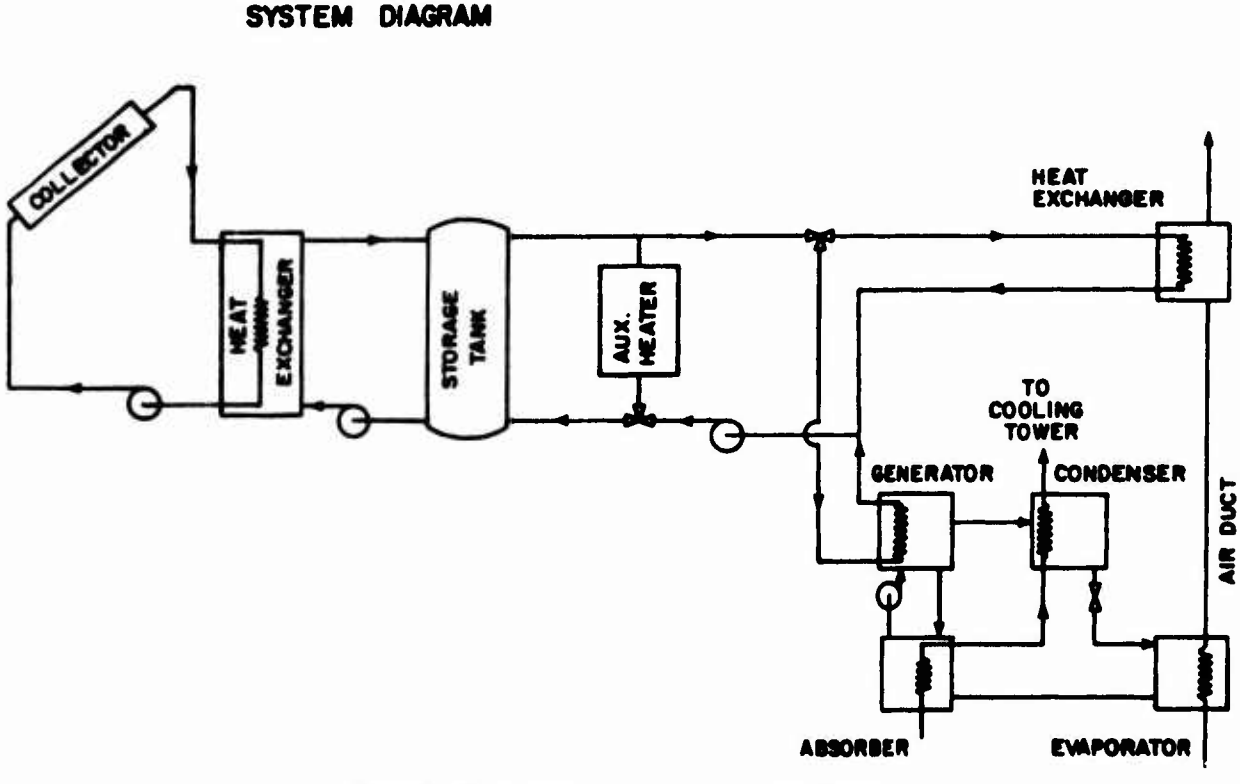

Figure 1. Solar heating and cooling system diagram.

they remain oriented toward the sun; i.e., tracking the sun. The collected energy's density can be further increased by using focusing, or other concentrating methods to intensify the sun's radiation on the collectors. Although this can result in heat of higher temperatures, means for tracking and concentrating are presently expensive. Consequently, this report will consider only fixed, flat-plate collectors.

Flat-Plate Collectors

Figure 2 is a cutaway sketch of a conventional flat-plate collector. The unit is mounted in a fixed position, and the metallic (copper, aluminum, or iron) absorber plate is coated to maximize solar energy absorption. Often, the coating has low emissivity in the infrared, which minimizes the re-radiation of energy from the hot absorber plate. Heat loss to the environment caused by conduction through the back of the collector is kept low by heavy insulation. The transparent cover plate reduces heat losses from convection, and by having low transmittance to infrared, reduces radiation losses. This design enhances the "greenhouse" effect and maintains a plate temperature which is much greater than ambient air temperature. Some models use two cover plates, separated by an air space, to further reduce convection loss, though this is at the expense of transmittance.

Useful heat is extracted from the collector by circulating air or a liquid over or through the absorber plate. Under favorable conditions, the heat energy removed can exceed 50 percent of the solar energy incident on the panel. For a given collector, efficiency is highest when the plate is coolest and when the difference between plate and ambient temperature is minimal.

High incident solar radiation and the absence of collector fluid circulation (stagnation) can cause the collector plate temperature to exceed 350°F (177°C). Thus, collector materials must be selected to withstand a wide temperature range and high thermal gradients.

Several manufacturers market solar collectors with wide-ranging collector performances and costs. The National Bureau of Standards has published a manual, NBSIR-74-635, which outlines test procedures designed to permit collector performance comparisons.[1]

Collector Fluids

The most common fluids used to transfer heat from the collector are air and water or water-glycol solutions. Liquid systems are generally preferred to air for combined heating and cooling systems, because less power is required for circulation; there are fewer problems with transmission and insulation (ducts vs. pipes); there is smaller storage mass and volume; and there is no commercially available cooling method which can directly use heated air.

[1] J. S. Hill and T. Kusuda, *Methods of Testing for Rating Solar Collectors Based on Thermal Performance*, NBSIR-74-635 (Thermal Engineering Systems Section, Center for Building Technology, National Bureau of Standards, December 1974).

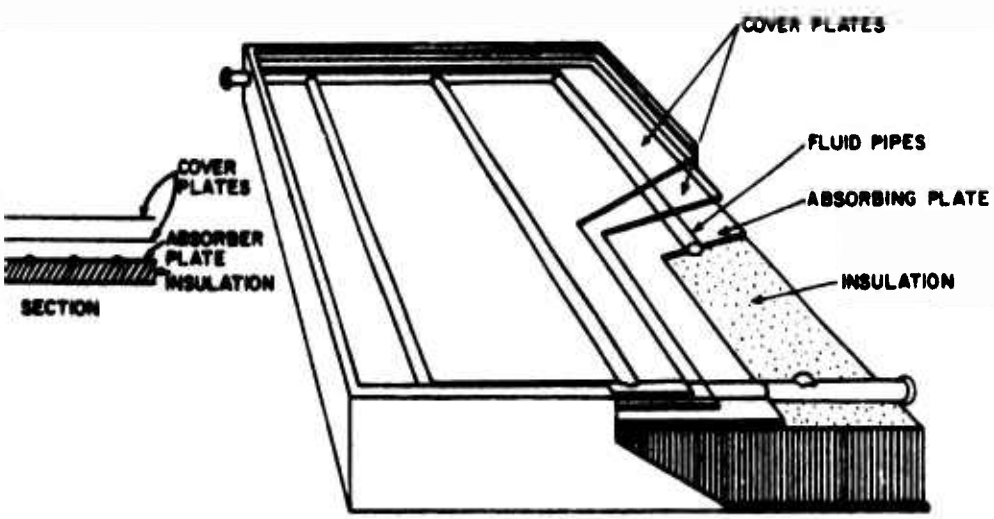

Figure 2. Conventional flat-plate collector.

Water may be circulated through collectors in locations where freezing does not occur, or in colder regions if the system is drained and flushed with inert gas whenever sufficient solar energy is not available; however, the most commonly used liquid is a water-glycol solution, buffered to reduce corrosion. In addition to decreasing the water's freezing point, the glycol increases its boiling point. This is an important advantage, since when the collector is operational its temperature can rise above 212°F (100°C). A relief valve and an expansion tank must be included in the collector system to insure its safe operation.

To reduce electrolytic corrosion, both within the collectors and elsewhere, piping of different metals must be isolated by fittings or by piping which is not electrically conductive. If a water solution is used, the pH must be monitored and buffers and inhibitors added periodically to suppress corrosion.

Other low-viscosity heat-transfer liquids, e.g., silicones, may deserve consideration as collector system fluids, because they can attain higher boiling points and possibly minimize corrosion problems.

Collector Location

The most common location for an array of collectors is the roof of the building to be heated or cooled. If the roof slope does not coincide with the desired collector tilt angle, the collectors should be spaced to insure that one row does not significantly shadow another at any time. If several buildings must be served, or if the roof area is too small, it may prove feasible to mount collectors on an unobstructed land area adjacent to the buildings being served. The collector array should generally be as close as possible to the energy-using facilities to minimize piping costs and heat loss, and to reduce pumping power requirements.

Collector Area

Since the cost of the collectors is a substantial portion of the total solar installation cost, the number of collectors (or the total useful collector area) must be carefully determined. The required collector area will be proportional to the load being met and to incident solar radiation, both of which vary according to site. Chapter 3 discusses determination of the collector area based on computer-derived curves.

Thermal Storage

Heat storage capacity is crucial in a solar installation design. Since the incident radiation on the collectors is only enough to be useful for a few hours each day, it is necessary to store heat so that it can accommodate part or all of the demanded load at night or during cloudy weather. Ideally, it would be desirable to store heat during a high radiation/low load period for delivery during a low radiation/high load period, i.e., season to season. Cost and size presently make such large storage capacities marginal, but storage capacity to handle one week's load now seems feasible.

Solar-derived heat may be stored either as sensible heat or as latent heat. Latent heat is used to melt a solid, such as Glauber salts or paraffin. Although such systems have small volume and mass, high cost and low reliability presently limit their use. Water is the best means of storing sensible heat, primarily because of its lower cost. To be useful, the water temperature must exceed the temperature demanded by the load—approximately 90°F (26.4°C) for heating, and 180°F (81.4°C) for absorption cooling. The upper temperature limit is the boiling point (212°F [100°C] at sea level). The tank may be made of metal, concrete, or fiberglass, depending on which is locally most economical. The surface-area-to-volume ratio can be minimized with a cylindrical tank whose diameter is equal to its height; for a tank with plane sides, a cube is best; a sphere is ideal.

The storage tank must be well-insulated so that heat loss through its walls will be very small in comparison to the heat delivered to the load. Since the surface-area-to-volume ratio becomes smaller with increasing tank size, the required insulation thickness is less for larger systems. Modern insulation materials, such as polyurethane foam, provide minimal heat loss at moderate cost.

The NBS report, *Method of Testing for Rating Thermal Storage Devices Based on Thermal Performance*, provides a method for evaluating storage systems.[2]

---

[2]G. E. Kelly and J. E. Hill, *Method of Testing for Rating Thermal Storage Devices Based on Thermal Performance*, NBSIR-74-634 (Thermal Engineering Section, Center for Building Technology, National Bureau of Standards, May 1975).

Heating

Conventional means are used to heat a building with stored solar energy. Hot water from the storage tank is pumped through a coil in the air-handling system, where the air is heated and delivered to the building. Unlike a conventional system, however, the water temperature varies considerably (80°F to 210°F [24.6°C to 81.4°C]); therefore, the fans, pumps, and coils must be capable of providing good heat exchange at the lower temperatures. The wide range of water temperatures makes radiators and baseboard convectors less attractive than forced, central air systems. Heat stored in the tank can also be used to heat or preheat water for domestic use in the building.

When the tank temperature drops below the minimum useful temperature, (usually about 80°F [29.6°C]), controls must be provided to turn on the auxiliary heater, which is usually a conventional gas, oil, or electrical heater. Since this auxiliary heat is expensive, controls and piping should be provided so that the water bypasses the storage tank when the auxiliary heat is in use.

Alternate heating methods may be used. A heat pump can provide heating at considerably lower tank temperatures; however, since solar energy cannot be used to drive the heat pumps for cooling, this method is suitable only for solar heating applications.

Cooling

Cooling a building by solar energy can be accomplished by several methods, including Rankine cycle, desiccant, and vapor absorption cooling.

Solar-powered Rankine cycle turbine engines have been used to drive conventional vapor compression cooling systems; however, these systems are experimental and prohibitively expensive, so they are not now considered to be a practical alternative.

A recently introduced prototype commercial desiccant system, designed to be powered by solar energy and natural gas, performs particularly well in dry climates; however, its performance coefficient in humid regions may be lower than that of absorption coolers. Since this system is not yet commercially available, it will not be considered in this report.

Lithium bromide and water vapor absorption cooling units which were originally designed for gas, steam, or hot water firing, have been developed to operate at generator temperatures as low as 180°F (81.4°C) with a coefficient of performance (COP) better than 0.65. These units are commercially available in limited sizes and have been successfully operated in solar installations. Manufacturers of large-capacity absorption chillers are beginning to examine the potential applicability of their equipment to solar-powered systems. Absorption cooling is currently the recommended method for cooling with solar energy, because it has been successfully demonstrated, and because it is currently the most inexpensive solar cooling method.

Reliability

The design of a solar installation must consider both reliability and maintenance cost. Since the solar collectors and the thermal storage tank are essentially static, maintenance costs and system reliability should be comparable with those of conventional heating and cooling systems. An NBS manual prepared for HUD, *Interim Performance Criteria for Solar Heating and Cooling Systems and Dwellings*,[3] provides some reliability criteria.

3 SYSTEM PERFORMANCE ESTIMATES

Simulation Study Procedure

In the past, selection or sizing of conventional heating and cooling systems was accomplished with relatively straightforward, steady-state, peak-load calculations. This method is still widely used to select boilers and chillers; however, solar energy systems differ from conventional systems in three key respects.

First, incident solar energy is not continuously available and may not be available at all during peak loads at night or in cloudy weather. Thus, since solar energy may not be able to meet all demands economically, provisions must be made for auxiliary energy supply systems. Sizing of solar system components is therefore based on annual system performance, rather than peak load calculations. The auxiliary system is still sized for peak loads.

[3] *Interim Performance Criteria for Solar Heating and Cooling Systems and Dwellings* (National Bureau of Standards, January 1, 1975).

Second, both the energy demand and the thermal energy storage mass influence the temperature of the fluid entering the solar collectors, and therefore influence the amount of incident solar energy that can be collected by a given collector array. Consequently, seasonal building heating and cooling load variations strongly influence the annual performance of a solar energy system.

Third, solar energy is typically collected and delivered over a large temperature range. This influences the performance of heating coils and absorption chillers. For these reasons, conventional "peak load" design methods are not acceptable, and computer simulation must be used.

To properly select solar system components; to establish optimum collector area, tank volume, and collector tilt and azimuth angle; and to determine the economic feasibility of a solar heating and cooling system, an accurate method of estimating the *annual* performance of a given solar energy system must be used. Such a method is provided by computer simulation techniques which use hourly weather data to predict hourly building heating and cooling loads, and the performance of candidate solar heating and cooling systems. The computer greatly facilitates the tedious task of estimating hourly building load profiles and performing the hourly iterative heat balance calculations required to estimate annual system performance.

It is recognized that load-predicting and solar energy system simulation programs are not yet readily available. Consequently, parametric computer simulation studies have been performed, and the results have been used to develop a method which *does not require the further aid of the computer* to estimate solar energy system performance for buildings. This method (described in Chapter 4) was developed by the following procedure:

(1) Two typical Army buildings and five geographical sites were selected for study.

(2) Hourly building load estimates were made for each building at each site, using hourly climatological data tapes from the National Climatic Center, National Oceanic and Atmospheric Administration (NOAA), Asheville, NC, and the National Bureau of Standards Load Determining Program (NBSLD). (Appendix B provides a general description of NBSLD.) Representative weather data years were selected for each site.

(3) Using hourly incident solar radiation data from the NOAA tapes and the hourly load estimates determined above, a series of parametric studies was performed by a solar system simulation program developed at the U.S. Army Construction Engineering Research Laboratory (CERL). These parametric studies provided performance estimates of the various solar heating and cooling systems. (See Appendix C for a detailed description of the CERL program.)

Building and System Simulation

The study investigated two structures of standard Army design which are typical of conventional office and dormitory buildings: a modular barracks and a two-battalion headquarters and classroom building.

The barracks (function category 72111) is a three-story, brick-faced masonry building having a flat, built-up roof and eight 3-man rooms on each floor. The 72-man modules are typically arranged in groups of three to five to form a larger barracks complex. (For this study, only one module was examined.) Each module contains approximately 4000 sq ft (372 m^2) of floor space. Ventilation was assumed to be by infiltration only.

The classroom and headquarters facility (function category 61041) is a single-story, brick-faced concrete block structure with a nearly flat, built-up roof. Approximately two-thirds of the floor space contains windowless classrooms. The remaining one-third, which is used as office space, has 20 exterior windows. This building contains approximately 12,000 sq ft (1115 m^2) of floor space.

Both buildings were assumed to comply with the 1 October 1972 DOD Construction Criteria Manual 4270. 1-M, which specified a unit thermal conductance minimum of .15 Btu/hr-sq ft (1.70 KJ/hr-m^2) for walls, .10 Btu/hr-sq ft (1.13 KJ/hr-m^2) for floors, and .05 Btu/hr-sq ft (.57 KJ/hr-m^2) for ceilings and roofs. The buildings were assumed to be heated only when the space temperature was 68°F (19.8°C) or below, and cooled only when the space temperature was 78°F (25.3°C) or above.

The buildings described above were analyzed for five sites chosen as being representative of the various

climate types in which there are large numbers of Army buildings: Fort Worth, TX (hot, sunny summers and mild winters); Los Angeles, CA (high insolation and relatively uniform temperatures throughout the year); Columbus, MO (moderately cold winters but summers, and moderate insolation); Madison, WI (cold winters, fairly short, warm summers); and Washington, DC (hot, humid summers, cool winters, and moderate insolation).

Figure 1 shows the configuration of the modeled solar heating and cooling system. Most simulations were performed for a single-cover, selective-surface collector. Sufficient simulations were made with other collectors to obtain a simple conversion factor to relate the performance of other collector types to the base type. (See the "Universal Curve for Estimating Solar Heating and Cooling Performance" section, page 15.) The thermal energy storage tank was assumed to be insulated with the equivalent of approximately 1 in (7.6 cm) of polyurethane insulation. A limited economy cycle was assumed in the calculations; outside air provided all cooling when its temperature was less than 55°F (12.6°C) for the headquarters, or less than 65°F (18.1°C) for the barracks.

Results of Simulation Studies

Table 1 shows the results of the load and solar simulation studies for the barracks module, and Table 2 shows results for the headquarters building. Values shown for optimum collector tilt angle were obtained from computer-derived curves, as shown in Figure 3.

Table 1

Barracks Module

SITE	FORT WORTH, TX	COLUMBIA, MO	MADISON, WI	WASHINGTON, DC	LOS ANGELES, CA
Year of Weather Data	1955	1965	1961	1954	1963
Latitude of Site in Degrees	32	39	43	39	34
Optimum Collector Tilt in Degrees	20	26	35	25	29
Annual Solar Radiation on Collector at Optimum Tilt (10^5 Btu/sq ft) (10^5 KJ/m^2)	6.54 (74.3)	6.03 (68.5)	6.23 (70.7)	5.64 (64.0)	6.68 (75.8)
Annual Horizontal Solar Radiation (10^5 Btu/sq ft) (10^5 KJ/m^2)	5.9 (67.0)	5.2 (59.0)	5.1 (58.0)	4.9 (55.6)	5.8 (65.0)
Annual Building Heating Load (10^8 Btu/yr) (10^8 KJ/yr)	0.008 (.008)	0.40 (0.42)	0.95 (1.00)	0.16 (.17)	~0 (~0)
Annual Building Cooling Load (10^8 Btu/yr) (10^8 KJ/yr)	-4.16 (-4.38)	-2.47 (-2.60)	-1.36 (-1.43)	-2.54 (-2.68)	-1.76 (-1.86)
Annual Thermal Energy Required for Absorption Cooling With COP= 0.65 (10^8 Btu/yr) (10^8 KJ/yr)	6.4 (6.7)	3.8 (4.0)	2.1 (2.2)	3.9 (4.1)	2.7 (2.8)
Total Annual Energy Required (10^8 Btu/yr) (10^8 KJ/yr)	6.4 (6.7)	4.2 (4.4)	3.03 (3.1)	4.15 (4.3)	2.70 (2.8)
Peak Heating Load (10^5 Btu/hr) (10^5 KJ/hr)	0.32 (.34)	0.89 (.94)	1.3 (1.4)	0.065 (.068)	~0 (0)
Peak Cooling Load (10^5 Btu/hr) (10^5 KJ/hr)	-1.42 (-1.44)	-1.30 (-1.36)	-1.20 (-1.27)	-1.36 (-1.43)	-1.28 (-1.35)

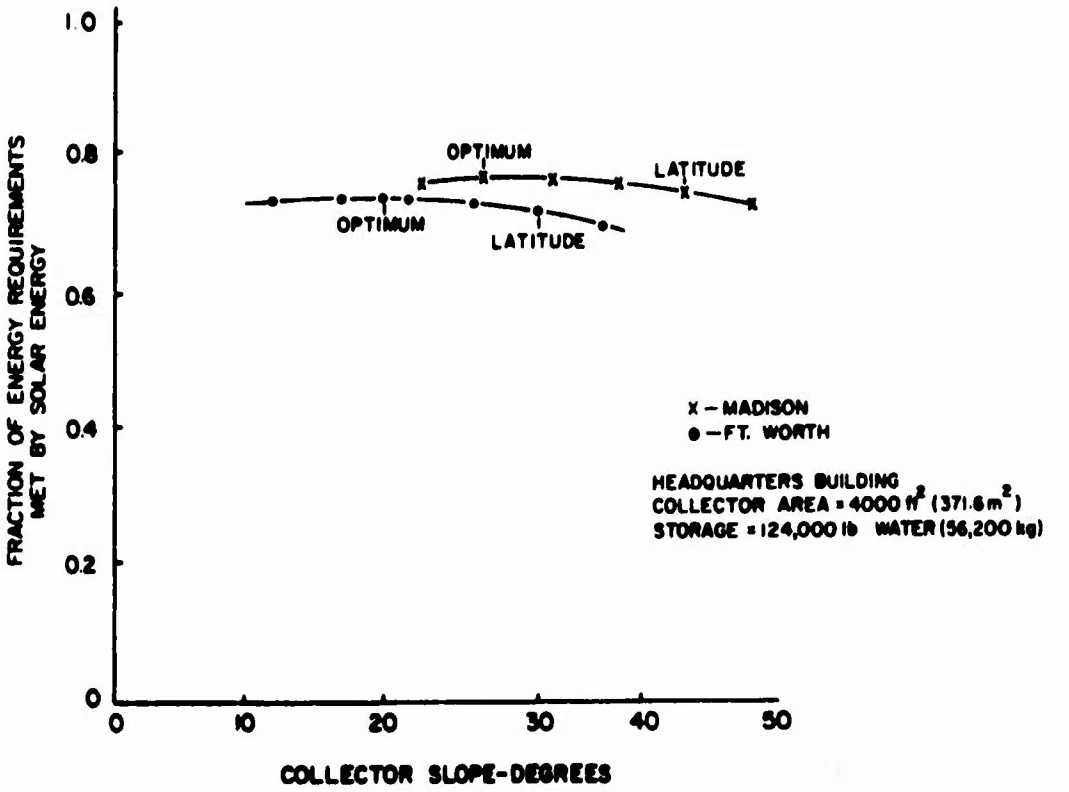

Figure 3. Effect of collector tilt angle on fraction of load met by solar energy.

Table 2

Headquarters Building

SITE	FORT WORTH, TX	COLUMBIA, MO	MADISON, WI	WASHINGTON, DC	LOS ANGELES, CA
Optimum Collector Tilt (Degrees)	22	28	28	27	31
Annual Solar Radiation on Collector at Optimum Tilt (10^5 Btu/sq ft) (10^5 KJ/m^2)	6.55 (74.4)	6.05 (68.7)	6.18 (70.2)	5.67 (64.4)	6.69 (76.0)
Annual Building Heating Load (10^8 Btu/yr) (10^8 KJ/yr)	0.4 (.4)	1.0 (1.1)	1.8 (1.9)	0.8 (.8)	0.4 (.4)
Annual Building Cooling Load (10^8 Btu/yr) (10^8 KJ/yr)	−7.7 (−8.1)	−5.3 (−5.6)	−3.5 (−3.7)	−5.0 (−5.3)	−5.7 (−6.0)
Annual Thermal Energy Required for Absorption Cooling With COP = 0.65 (10^8 Btu/yr) (10^8 KJ/yr)	11.9 (12.5)	8.1 (8.5)	5.4 (5.7)	7.7 (8.1)	8.8 (9.3)
Total Annual Energy Required (10^8 Btu/yr) (10^8 KJ/yr)	12.34 (13.0)	9.08 (9.5)	7.21 (7.6)	8.52 (9.0)	9.19 (9.7)
Peak Heating Load (10^5 Btu/hr) (10^5 KJ/hr)	--	0.58 (.61)	0.89 (.94)	0.24 (.25)	--
Peak Cooling Load (10^5 Btu/hr) (10^5 KJ/hr)	−3.0 (−3.2)	−2.9 (−3.0)	−2.8 (−2.9)	−2.9 (−3.0)	−2.8 (−2.9)

These curves show that the tilt angle is not critical; a deviation of ±5° from optimum has little effect on performance. It is interesting to note that when the collector has an appropriate tilt, latitude is not a dominating factor affecting annual incident radiation.

At all sites, even the coldest, the cooling load exceeds the heating load. The line in Tables 1 and 2 labeled "Annual Thermal Energy Required for Absorption Cooling With COP = 0.65" is the thermal energy required by the absorption cooler to meet the building cooling load. Adding the heating load to this value gives the total annual thermal energy required.

Figures 4-8 are plots of the solar performance curves for the barracks module of each sample site. The ordinate on each graph is the fraction of the total annual thermal load supplied by solar energy for the particular site. The abscissa is the total effective collector area. Each graph has four curves corresponding to different ratios of storage water mass to collector area M_s/A_c, where M_s is in pounds of water and A_c is in square feet. (One lb of water per square foot of collector area corresponds to 4.9 kg of water per square meter of collector.) These curves are representative of the type of performance curve that must be constructed to permit determination of the economic feasibility of solar heating and cooling.

Figure 9 compares the solar-supplied energy for different sites for an arbitrarily selected storage capacity of 31 lb water per square foot of collector area (152 kg/m^2). It can be seen that for a system of given size, the amount of solar-supplied energy ranges greatly for the different sites, with Fort Worth having the greatest amount and Los Angeles the smallest. These differences are largely due to the differences in total annual thermal energy demanded by the building at each site and indicate the critical impact of building energy use on the overall performance of the solar energy system. Figure 10 is an example of how the fraction of load provided by solar energy depends on the thermal storage mass, with collector area as a parameter. These curves show a big improvement for increasing storage from 8 to 16 lb water/sq ft (38 to 304 Kg/m^2) and only minor improvement for increasing storage from 31 to 62 lb/sq ft (152 to 304 Kg/m^2).

Figures 11 to 15 are performance curves for the headquarters building for the five sample sites. The format is the same as the curves for the barracks module. Figure 16 is a comparison of the sites.

Universal Curve for Estimating Solar Heating and Cooling Performance

Figure 17 is a dimensionless comparison of both buildings at all sites. The abscissa is the incident annual radiation on the collector with optimum tilt (the product of collector area and radiation density) divided by the total annual energy requirements. The ordinate is the fraction of this annual energy requirement met by solar energy. This plot is for a storage of 16 lb water per square foot of collector area. The simulation data points fall remarkably close to the single representative curve shown. Thus, Figure 17 can provide a reasonably good approximation of solar heating and cooling system performance for all buildings at all sites. Figures 18 and 19 are similar plots with representative curves for larger storage sizes. Figure 20 shows the three representative curves. The constants were obtained by a computer determination of the best "least square" fit of the simulated data.

Each curve is described by the general equation

$$\rho = B(r - 0.082\, r^2) \qquad \text{(Eq 1)}$$

where ρ is the fraction of the annual load supplied by solar energy, and r is a dimensionless parameter defined by

$$r = \frac{H_\theta A_c}{Q_L M} \qquad \text{(Eq 2)}$$

where:

H_θ is the annual radiation energy per unit area on the tilted collector,

A_c is the collector area,

M is the multiplying factor of Table 3, and

Q_L is the total annual energy requirements.

The constant B, whose values are shown in Figure 20, depends on the chosen storage size.

If values for H_T, Q_L, B, and M are known, Eq 1 reduces to ρ as a function of the collector area, A_c, alone—the same form as the performance curves shown earlier. This equation can then be used for economic feasibility calculations.

The annual radiation density on the tilted collector surface H_θ may be obtained by using the empirically

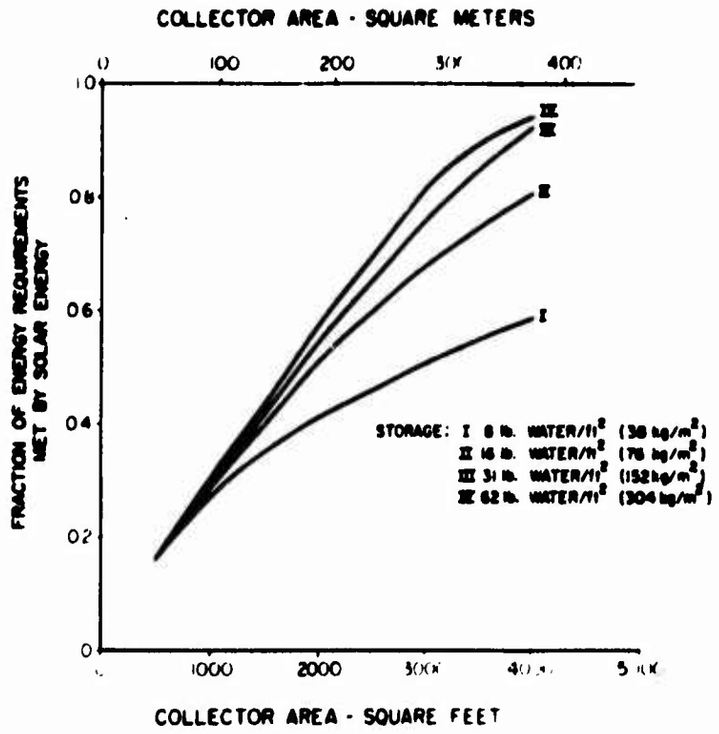

Figure 4. Performance curve for barracks at Fort Worth, TX, with total annual energy requirement of 6.4×10^8 Btu (6.7×10^{11} joules).

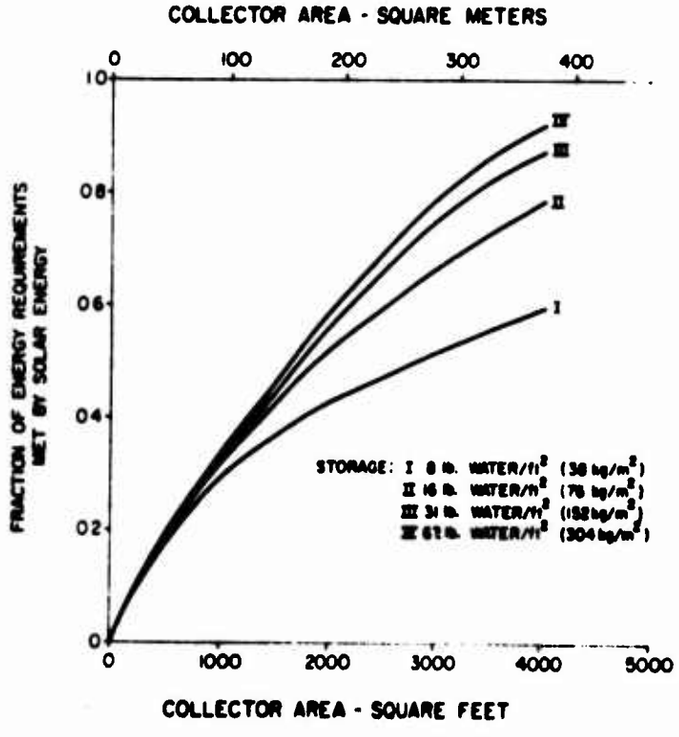

Figure 5. Performance curves for barracks at Washington, DC, with total annual energy requirements of 4.05×10^8 Btu (4.27×10^{11} joules).

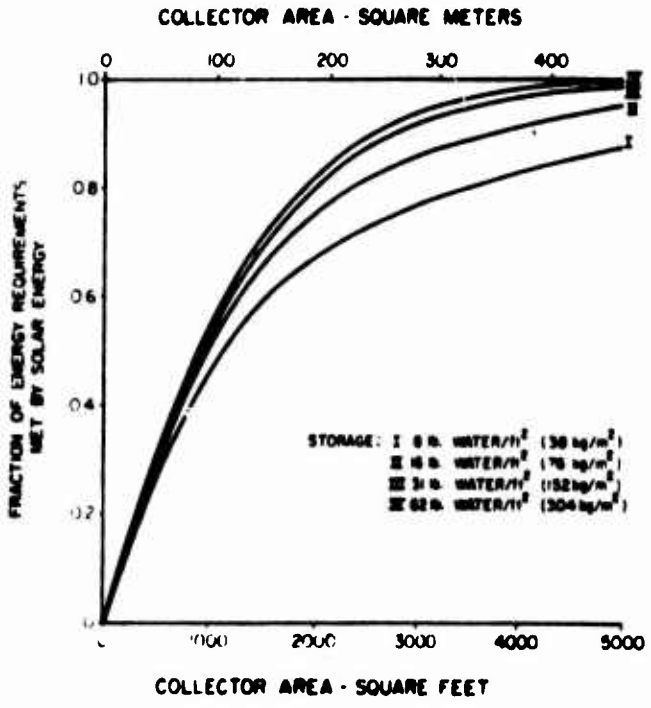

Figure 6. Performance curves for barracks at Columbia, MO, with total annual energy requirements of 4.2×10^8 Btu (4.4×10^{11} joules).

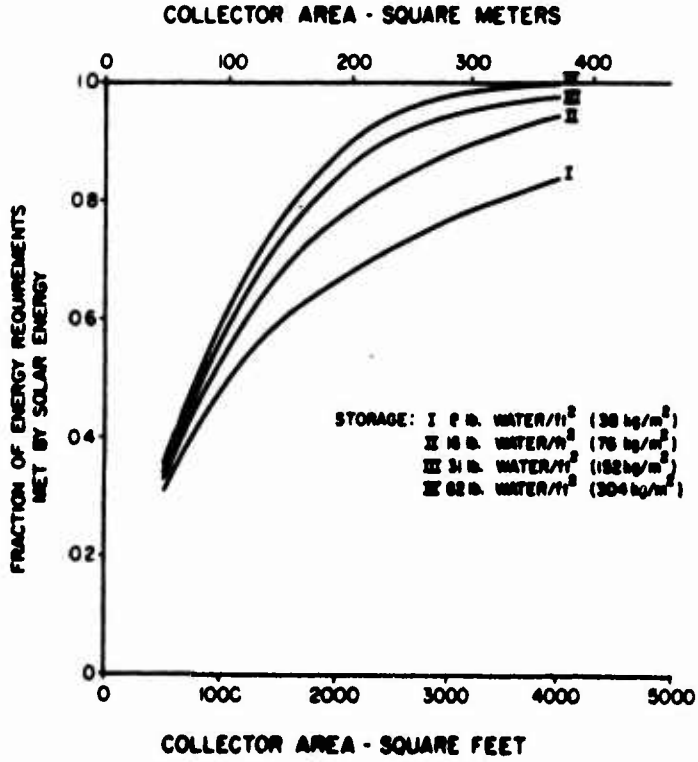

Figure 7. Performance curves for barracks at Madison, WI, with total annual energy requirements of 3.03×10^8 Btu (3.20×10^{11} joules).

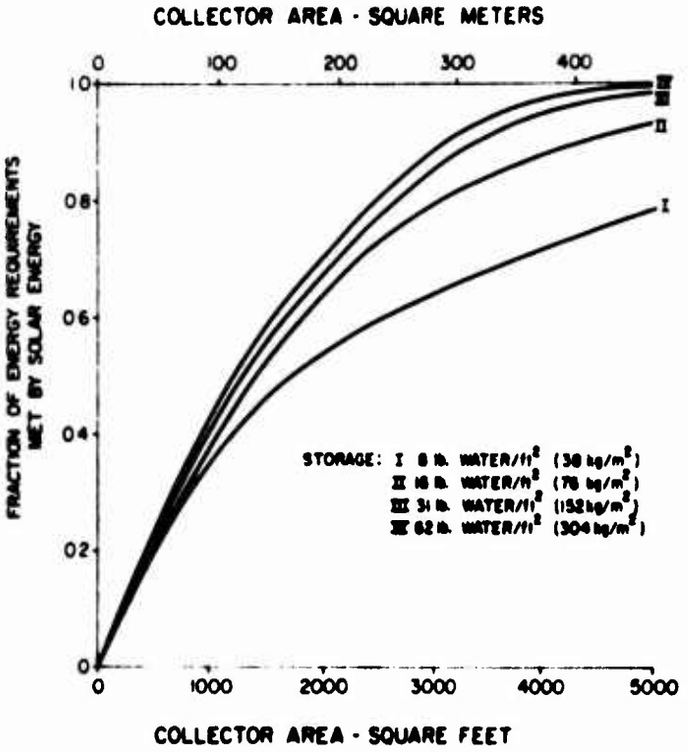

Figure 8. Performance curve for barracks at Los Angeles, CA, with total annual energy requirements of 2.7×10^8 Btu (2.85×10^{11} joules).

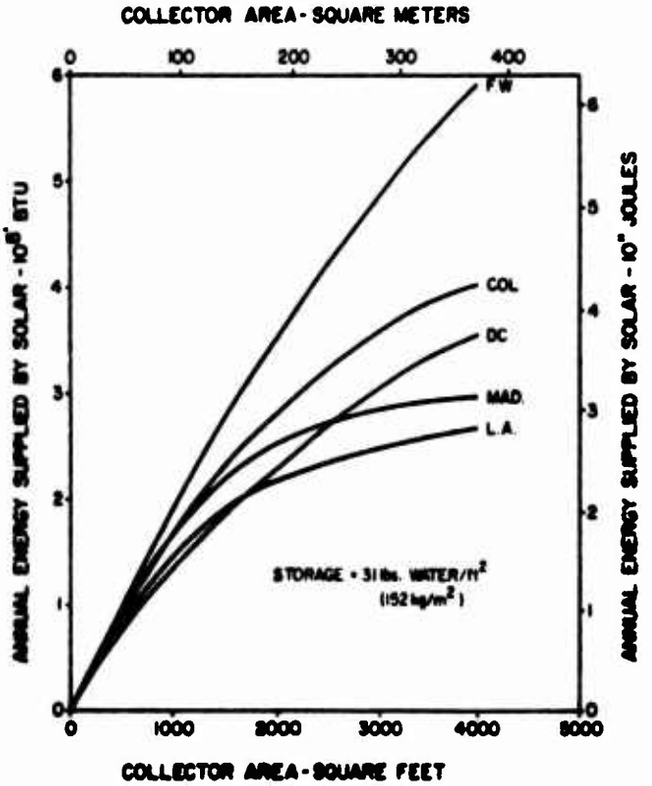

Figure 9. Comparison of performance curves for barracks at all sites.

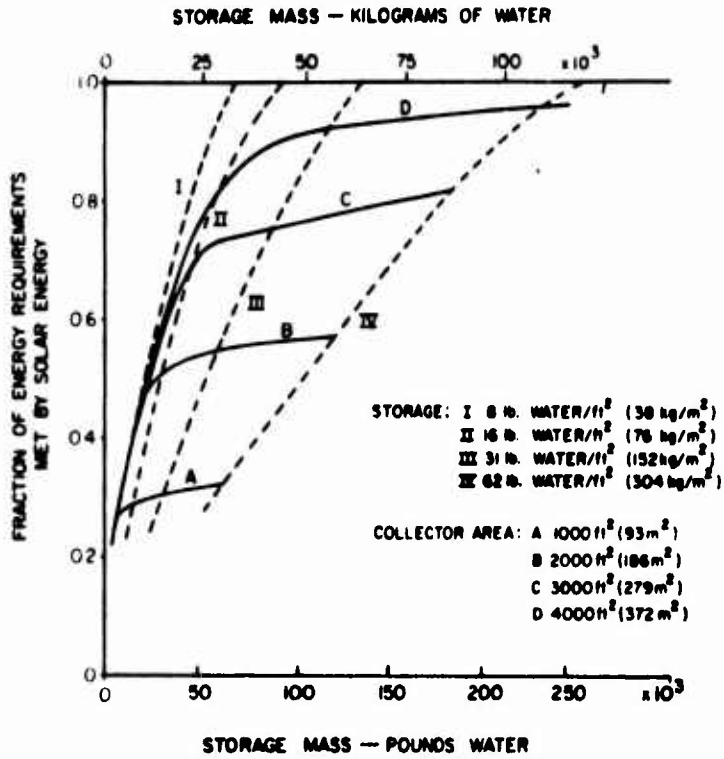

Figure 10. Effect of thermal storage capacity on performance.

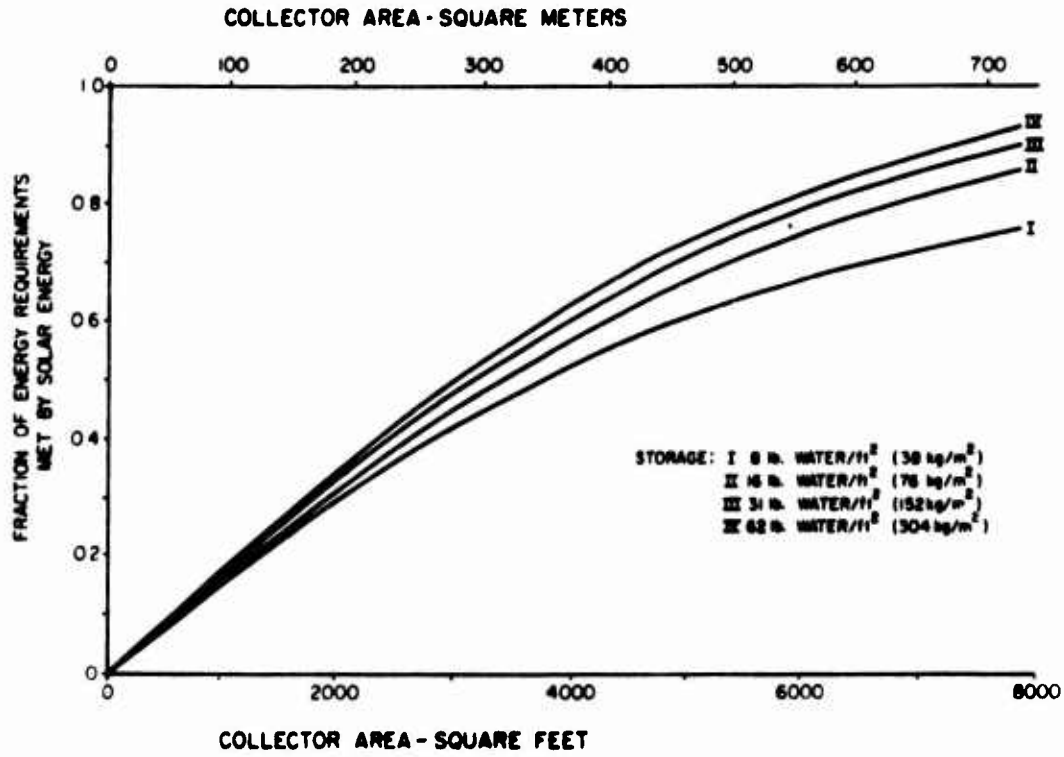

Figure 11. Performance curves for headquarters building at Fort Worth, TX, with total annual energy requirements of 12.34×10^8 Btu (13.02×10^{11} joules).

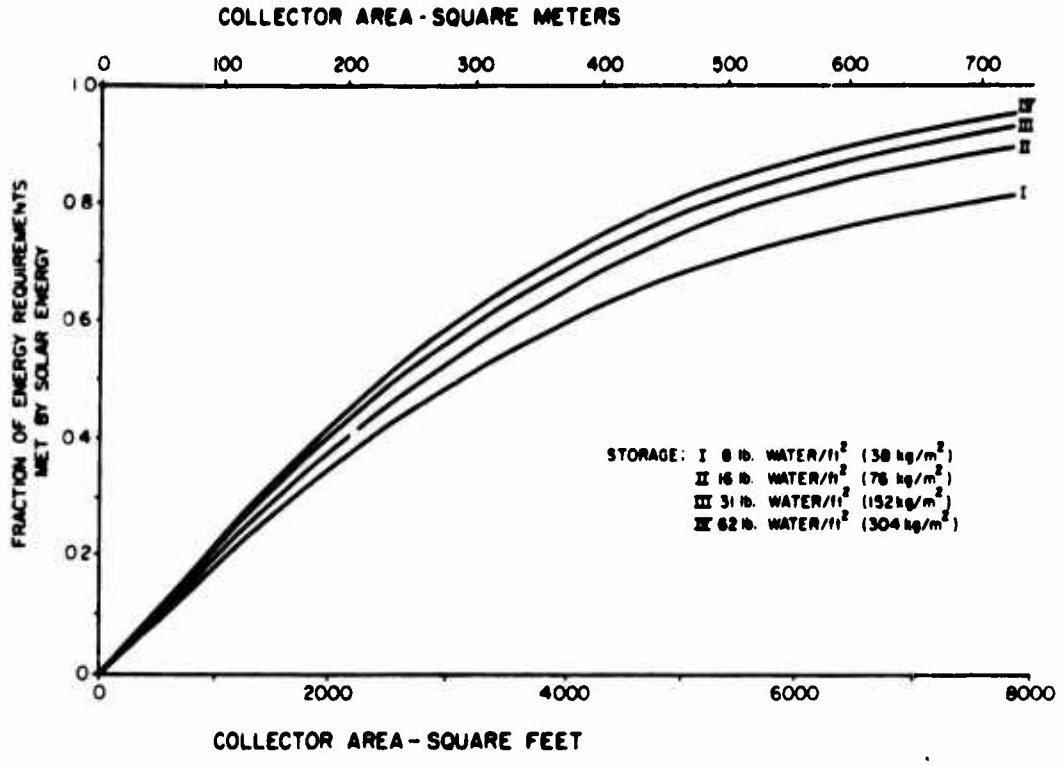

Figure 12. Performance curves for headquarters building at Columbia, MO, with total annual energy requirements of 9.08×10^8 Btu (9.58×10^{11} joules).

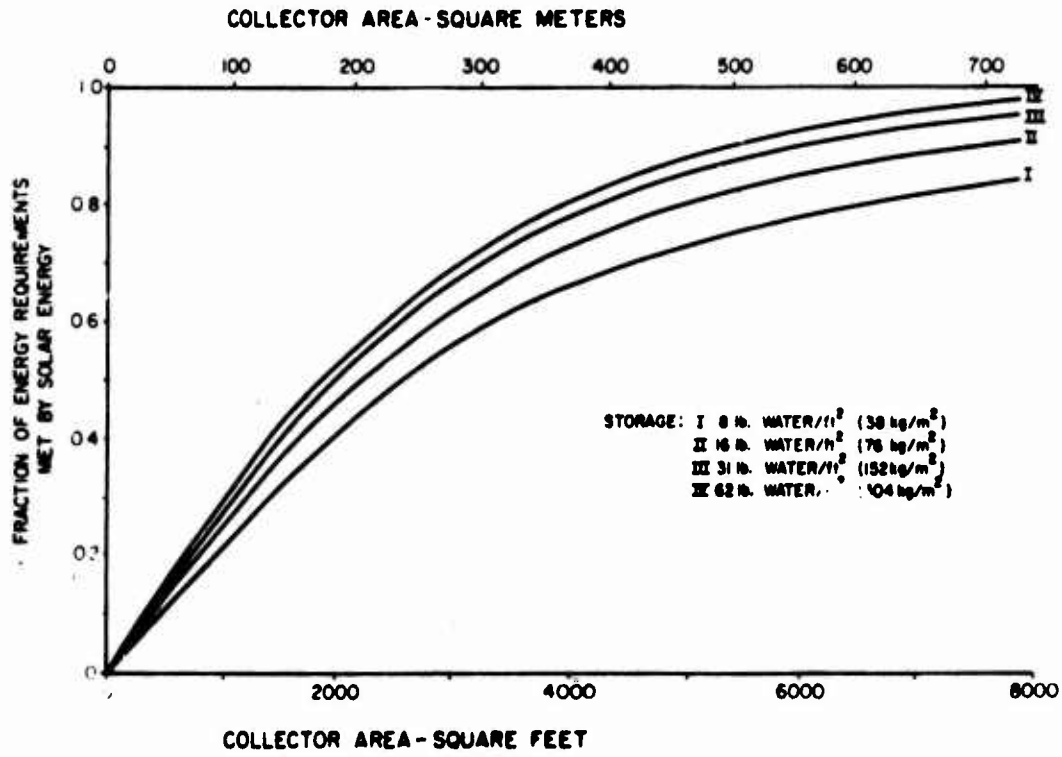

Figure 13. Performance curves for headquarters building at Madison, WI, with total energy requirements of 7.21×10^8 Btu (7.61×10^{11} joules).

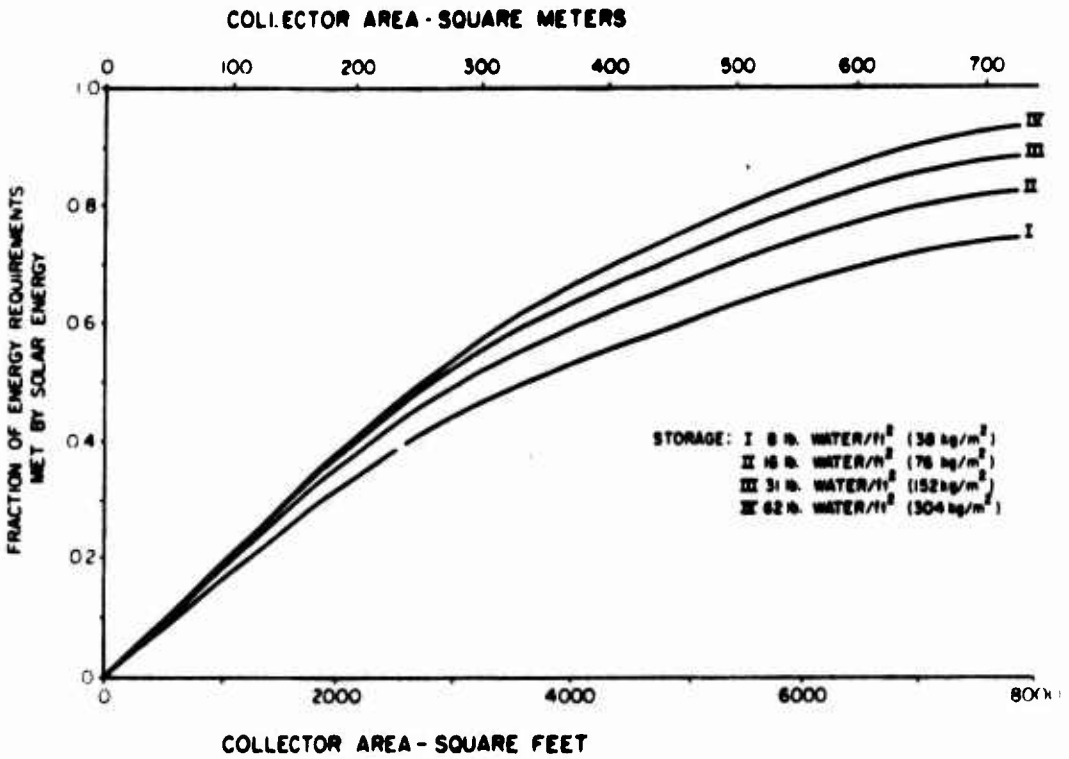

Figure 14. Performance curves for headquarters building at Washington, DC, with total annual energy requirements of 8.52×10^8 Btu (9.0×10^{11} joules).

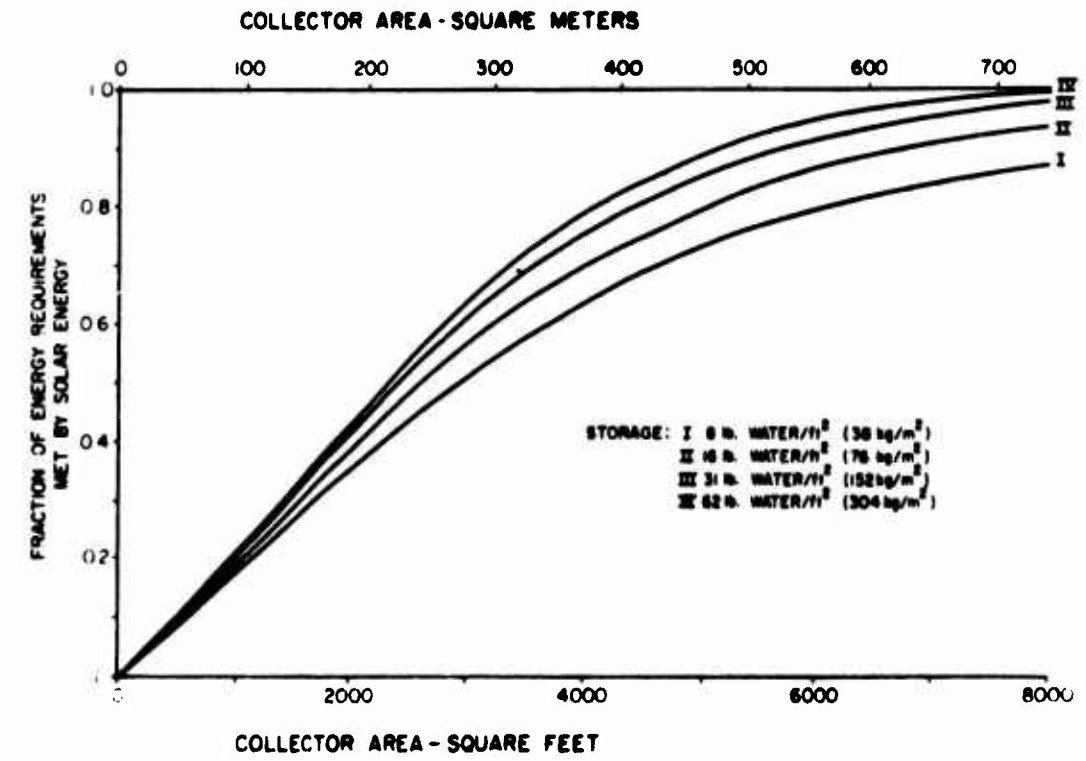

Figure 15. Performance curves for headquarters building at Los Angeles, CA, with total annual energy requirements of 9.19×10^8 Btu (9.7×10^{11} joules).

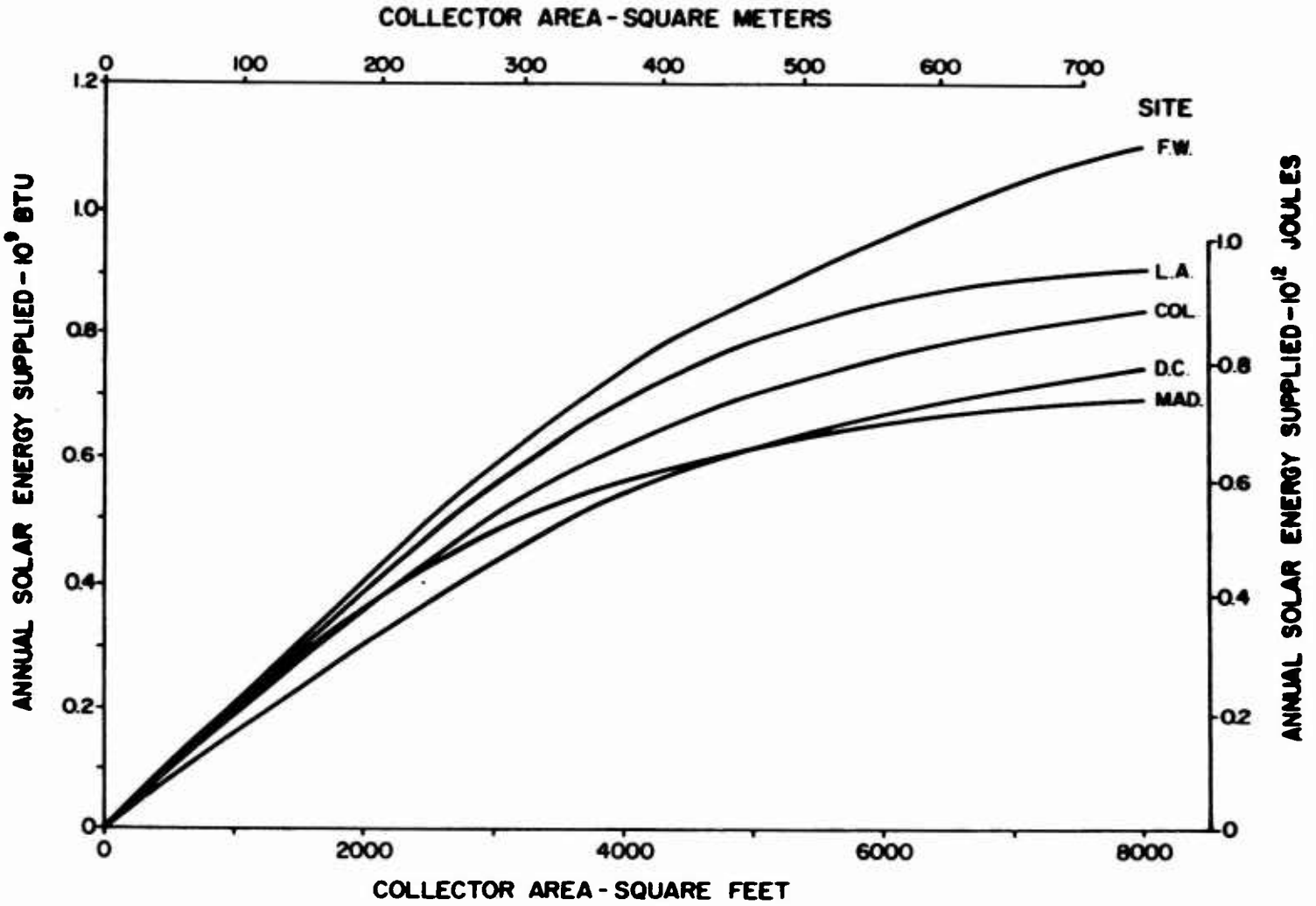

Figure 16. Comparison of performance curves for headquarters building at all sites with storage = 31 lb water/sq ft ($152 kg/m^2$).

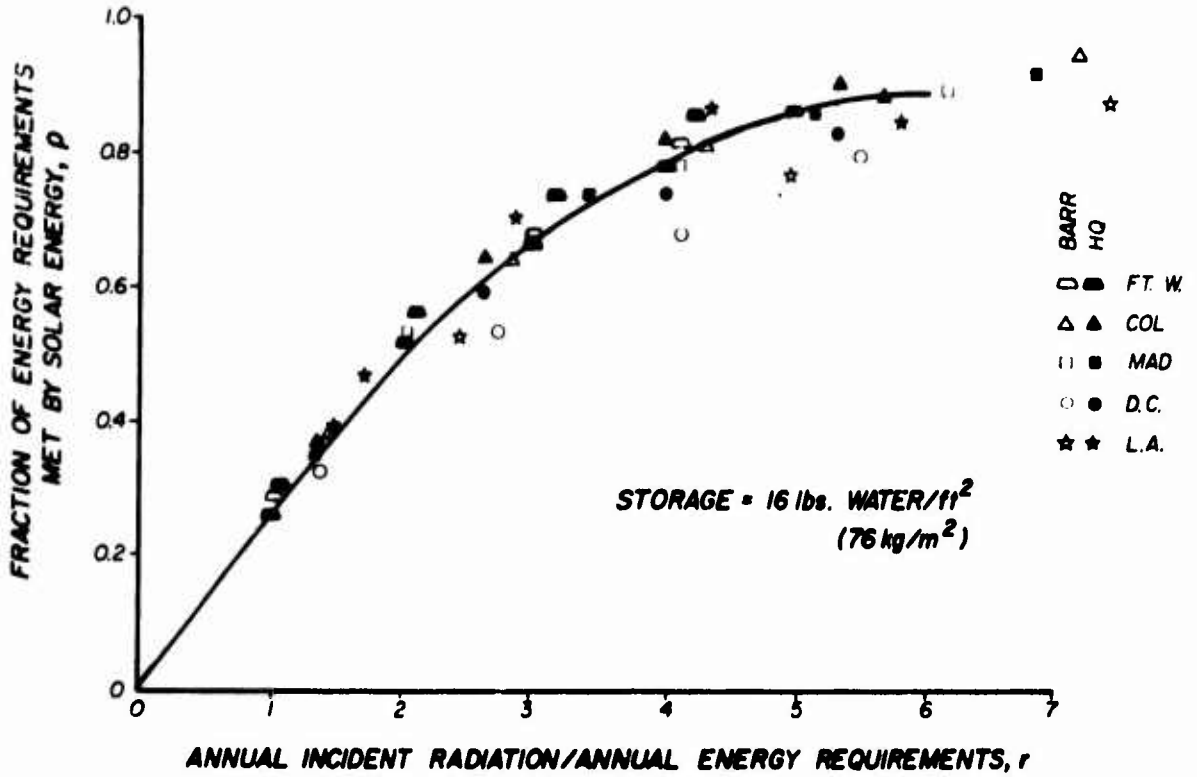

Figure 17. Universal performance curve for both buildings at all sites. Storage = 16 lb water/sq ft (76 kg/m^2).

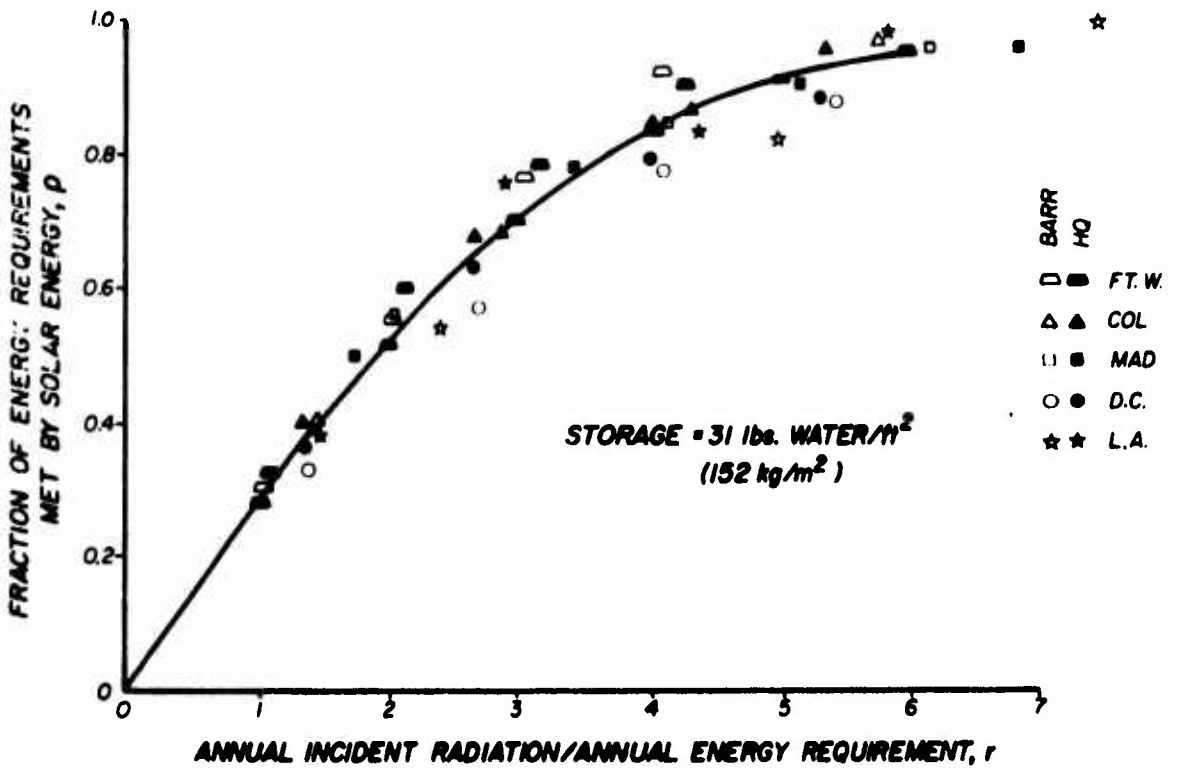

Figure 18. Universal performance curve for both buildings at all sites. Storage = 31 lb water/sq ft (152 kg/m^2).

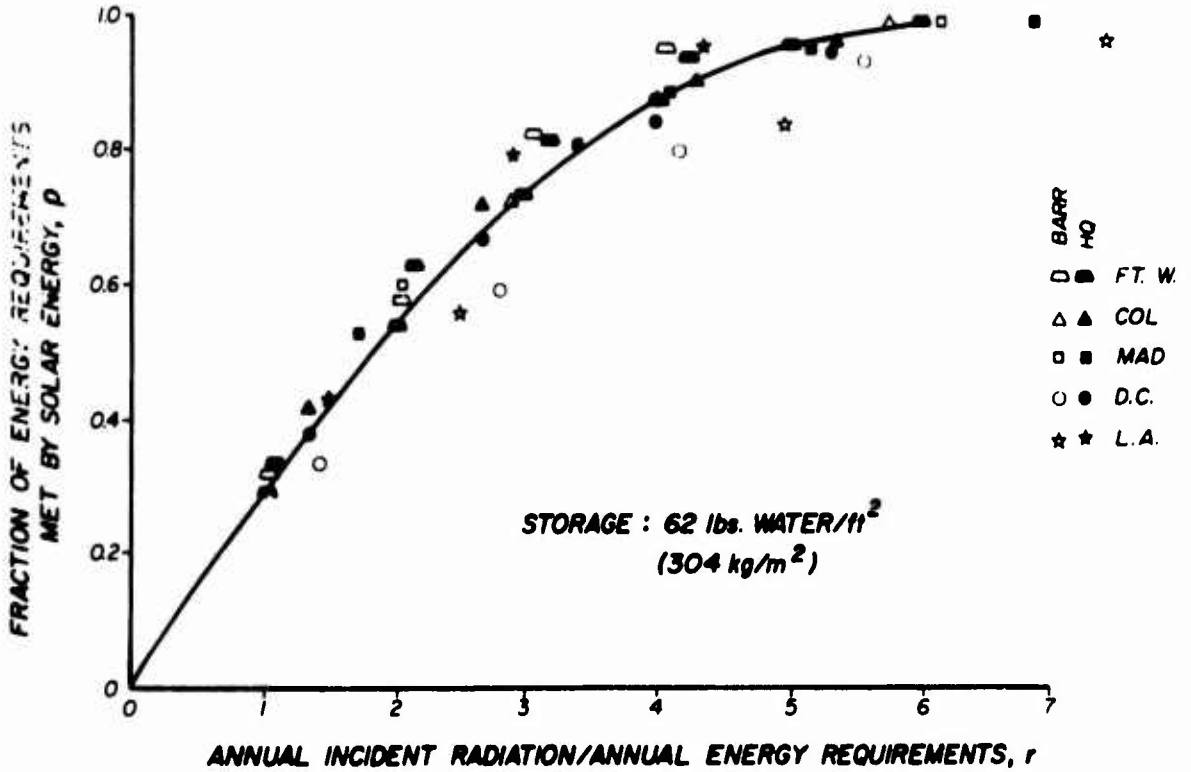

Figure 19. Universal performance curve for both buildings at all sites. Storage = 62 lb water/sq ft (304 kg/m^2).

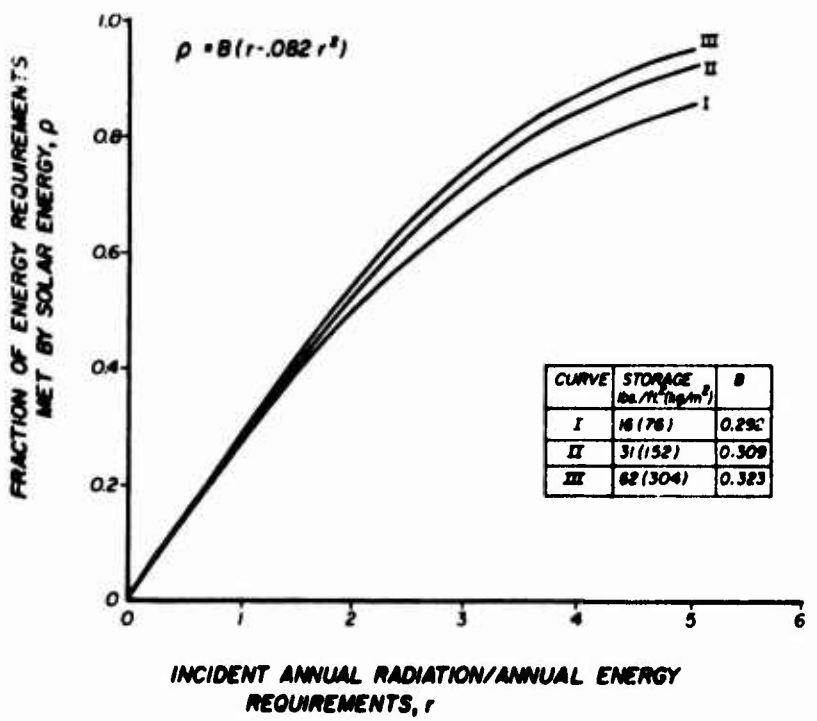

Figure 20. Approximate universal performance curves for three storage volume-to-collector area ratios obtained from the analytic expression shown.

derived formula

$$H_\theta = \frac{H_o}{\cos(\theta_L - 8)} \qquad \text{(Eq 3)}$$

where:

H_o is the annual radiation density on a horizontal surface and is available for most regions in the United States, and

θ_L is the latitude of the chosen site.

A map of mean daily horizontal radiation, taken from the Climatic Atlas of the United States (U.S. Dept of Commerce) is shown in Figure 21. The radiation density is given in Langleys/day. The annual radiation density H_o in Btu/sq ft is obtained by multiplying the value from the map by 1.34×10^3; to obtain H_o in joules/m^2, the factor is 1.53×10^7.

The problem of determining the annual heating and cooling load, Q_L, is addressed on p 27.

Since all the simulations were made with a collector of particular design (single cover with selective coating; α=0.90; ϵ=0.10, n=1), a comparison is made in Table 3 for collectors with other properties. In Table 3 α is the absorptivity of visible radiation of the absorbing plate, and ϵ is the infrared emissivity of the plate. Values of α and ϵ are available from the collector manufacturer. The values in the table are the multiplying factor, M, used in Eq 2 to obtain performance curves.

By using the curves of Figure 20 in conjunction with the adjustment factors for collector type, buildings and site-specific curves can be constructed which show the fraction of annual load met from solar energy as a function of collector area. Separate curves of this type can be drawn for different storage mass to collector area ratios, as illustrated by Figures 1 through 8 and 11 through 15, and for different collector types. Such curves permit determination of economically optimum designs, as will be described in Chapter 4.

It should be noted that for buildings with dominant cooling loads, if the annual heating and cooling load of the building and the annual radiation density of the site are known, the previously described performance estimating method can be applied regardless of the type of building or site. However, the method applies only to systems designed to meet *both heating and cooling loads*. The curves do not apply to heating only applications or to applications which have small cooling loads. Such curves are being prepared and will be available in the near future.

An example will illustrate how the universal curves of Figure 20 may be used to determine the performance of a solar installation. Consider a building at Nashville, TN, which is known to have an annual heating load of 1×10^8 Btu and an annual cooling load of 4×10^8 Btu. The thermal requirement for the cooling is then $4 \times 10^8/0.65 = 6.15 \times 10^8$, where 0.65 is the coefficient of performance of the absorption cooler. The total annual energy requirement, Q_L, is then $1 \times 10^8 + 6.15 \times 10^8 = 7.15 \times 10^8$ Btu.

From the map for solar radiation (Figure 21), we find that for Nashville, the horizontal radiation density is 355 Langleys/day, and the latitude is about 32°. H_o is then equal to $355 \times 1.34 \times 10^3 = 4.8 \times 10^5$ Btu/sq ft

Table 3

Collector Area Multiplying Factor, M

COLLECTOR AREA MULTIPLYING FACTORS FOR DIFFERENT COLLECTOR DESIGNS

α		0.96	0.94	0.90
ϵ		0.96	0.30	0.10
N	1	1.55	1.09	1
	2	1.09	0.97	0.93

α = ABSORPTIVITY

ϵ = EMISSIVITY

N = NUMBER OF GLASS COVERS

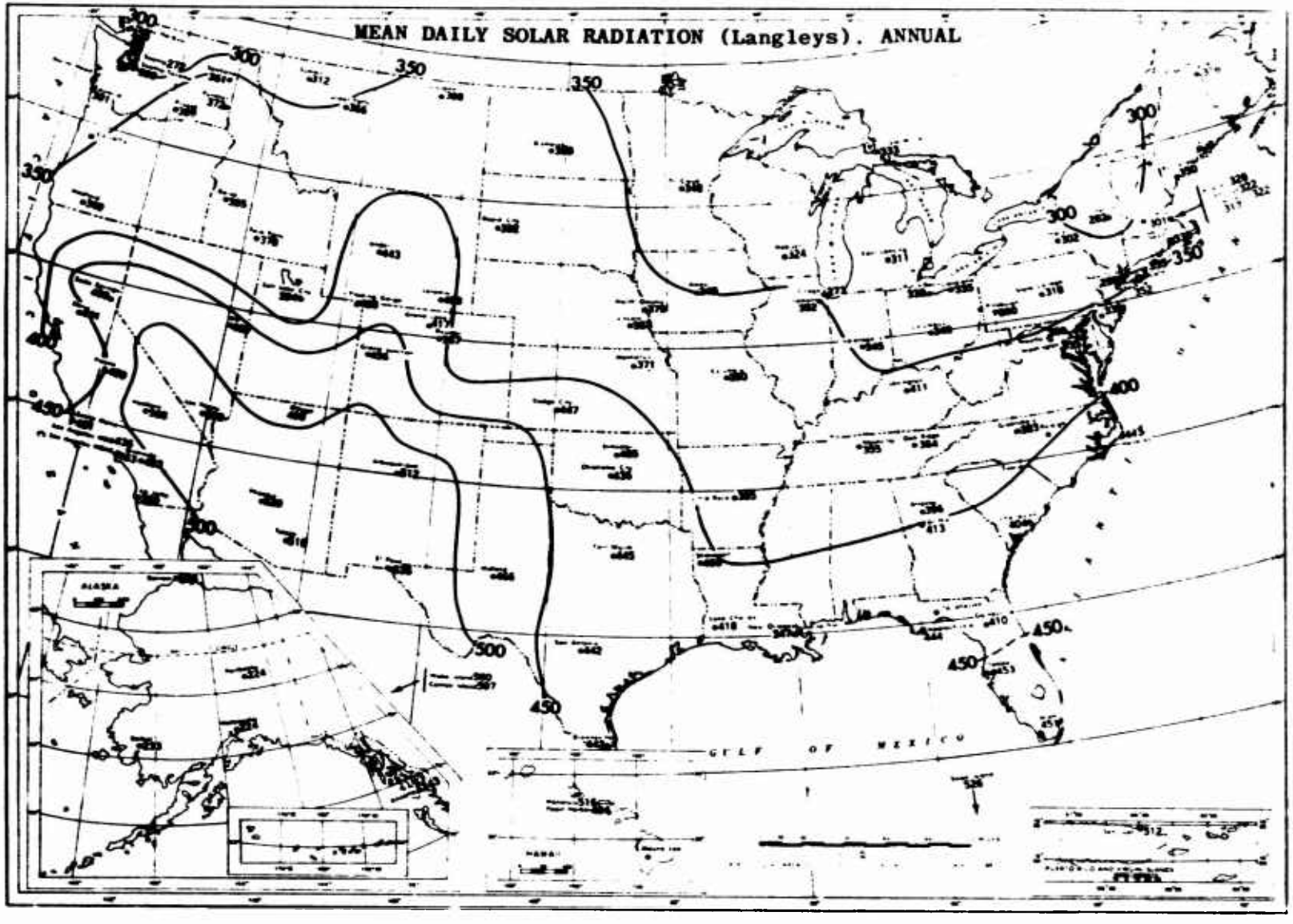

Figure 21. Solar radiation map of U.S. From *Climatic Atlas of the United States* (U.S. Department of Commerce, 1968).

annually. Using Eq 3, the radiation density on the tilted collector, H_θ is found.

$$H_\theta = \frac{4.8 \times 10^5}{\cos(32 - 8)} = 5.25 \times 10^5 \text{ Btu/sq ft}$$

From Eq 2, assuming M=1 (single cover, selective coating), we determine

$$r = \frac{5.25 \times 10^5 A_c}{7.15 \times 10^8} = 7.34 \times 10^{-4} A_c$$

Using this relation, Eq 1, and Figure 20, and selecting a storage of 31 lb/sq ft (151 kg/m^2) the fraction of the energy requirements supplied by solar gives energy:

$$\rho = 0.309 [7.34 \times 10^{-4} A_c \quad 0.082 (7.34 \times 10^{-4} A_c)^2]$$

$$= 2.27 \times 10^{-4} (A_c - 6.02 \times 10^{-5} A_c^{\,2})$$

Table 4 shows values of ρ for a range of collector sizes.

Table 4

Energy Requirements Met by Solar Energy

A_c (sq ft)	500	1000	1500	2000	2500	3000	3500
ρ	0.11	0.21	0.31	0.40	0.48	0.56	0.63

The table contains the performance data needed to make an economic feasibility assessment.

Determining Annual Heating and Cooling Energy Load

It is not the objective of this report to provide a method for precise determination of annual building heating and cooling energy requirements; however, the problem must be briefly addressed because of its impact on solar energy system economic feasibility assessment.

For sites and buildings other than those for which annual energy requirements are given in the "Results of Simulation Studies" section, p 13, the annual building heating and cooling energy requirements can best be estimated from measured consumption data for identical or similar buildings near the building being considered. When this is not possible, hourly load-predicting computer programs which use actual weather data are the next best choice. The NBSLD Program (Appendix B) and NASA's "NECAP" Program provide good results. If other programs requiring the input of peak heating and cooling loads are used, these loads should be calculated with response factor methods outlined in the ASHRAE *Handbook of Fundamentals*, 1973 edition.

When the techniques described above are not available, a rough approximation of the heating and cooling load can be obtained by scaling the results presented in the "Results of Simulation Studies" section. The first step in this scaling procedure is to adjust for sites not located at or near the five studied. Various approaches have been suggested for adjusting the annual heating and cooling load to account for climate differences. Most correlations, however, have been poor. In particular, peak heating and cooling loads have little or no relationship to geographical differences in annual energy consumption. Degree days, particularly "cooling degree days" are also poor adjustment factors. Therefore, intuitive adjustments based on information discussed in the "Results of Simulation Studies" section appear to be the best recourse. Interpolation, weighted by judgment, between annual loads for the two sites closest in *climate* to the location being considered appears to be the best approach. For example, for estimating the annual load of a barracks in central Illinois, interpolation between the loads of Columbia, MO and Madison, WI, should produce a reasonable result.

When site adjustments have been made, adjustments for differences in building size or configuration must be accomplished. Note that the buildings selected for the computer simulation study were chosen because they typify two of the major functional building types found at Army posts, (i.e., troop housing and administrative buildings) and are representative, in terms of their thermal responses, of most concrete masonry and brick construction. Consequently, the results of the energy requirement calculations for two buildings at five sites presented in the "Results of Simulation Studies" section, (p 13), may be legitimately extended to other masonry and brick construction by applying a rough scaling factor based on the ratio of the sum of roof and exterior wall area of a candidate building to that of one of the buildings studied. This scaling should *not* be applied, however, to lightweight or uninsulated

buildings or to buildings with large glass areas, since the thermal properties of these buildings differ largely from those studied.

Note that regardless of the method used to determine the annual building energy requirements, the value required to implement the procedures discussed in the "Universal Curve" section is *not* the sum of the absolute values of the annual building heating load and the annual cooling load; it is rather the amount of energy required by the heating and cooling systems to meet the building load (note the difference between cooling loads and energy required for cooling in Tables 1 and 2). This distinction is critically important, not only because of the coefficient of performance penalty associated with absorption cooling, but also because large energy consumption differences can occur between different types of fan systems when meeting identical building loads (compare, for example, two-pipe fan coil versus terminal reheat systems).

This leads to another general rule which must be considered in the application of solar energy. It is currently more cost-effective, in almost every case, to apply strict energy conservation techniques to a building before considering solar energy as an alternative means of heating and cooling it. The application of solar energy should therefore be considered in its proper perspective as one of many mutually compatible energy conservation options.

4 ECONOMIC FEASIBILITY ASSESSMENT AND SELECTION OF OPTIMUM SYSTEM

The method described in this chapter for defining the economically optimum solar energy system relies both on the building's annual energy consumption (p 27) and on the solar energy system performance estimates (p 15) described in Chapter 3. The procedure is an adaptation of that suggested by Butz, et al.[4] and leads to the selection of a collector area and tank volume which will maximize the "trade-off" between solar energy system costs and fuel cost savings. The method relies on a simple graphical comparison of the life-cycle (present worth) cost difference between a solar energy system and a conventional system. Appendix A provides an example application of the method to a battalion headquarters and classroom building at Fort Hood, TX.

The first task is estimation of the life-cycle cost of the solar energy system components. Because this method is comparative, only the costs of components that are not normally part of a conventional heating and cooling system should be considered; thus, the cost of the building's air-handling system would not be considered, but the difference between the installation cost of a more expensive absorption chiller and of a less expensive centrifugal chiller should be charged to the solar energy system. Note that for a solar heating and cooling system, certain cost elements vary according to the size of solar energy systems, and others are relatively fixed, regardless of the collector area or tank volume chosen. Collector and storage tank costs are obvious examples of system-size-dependent items; other examples include heat exchanger costs, and certain pump and piping costs. The additional control system cost associated with a solar energy system is an example of a cost difference that is largely independent of collector area. The cost difference associated with the purchase and installation of an absorption chiller is also relatively independent of solar collector area, since for all but the smallest solar collector areas, selection of an appropriate absorber is dictated by the peak building cooling load.

When these fixed and variable cost items are separated, it is a relatively straightforward matter to estimate the life-cycle cost difference between solar and conventional heating and cooling systems for various collector area/storage capacity combinations. Figure 22 illustrates how the capital component of the life-cycle cost increases with collector area.

The second step of the comparison procedure is establishment of the life-cycle fuel costs for conventional and solar energy systems of varying sizes.

For the conventional system, annual fuel costs can be estimated as follows:

(1) Determine the annual heating and cooling energy loads for conventional equipment, using the procedures discussed in Chapter 3, p 27.

(2) Convert the cooling energy load to kilowatt

[4] L. W. Butz, et al., *Use of Solar Energy for Residential Heating and Cooling*, M. S. Thesis in Mechanical Engineering (University of Wisconsin, 1973).

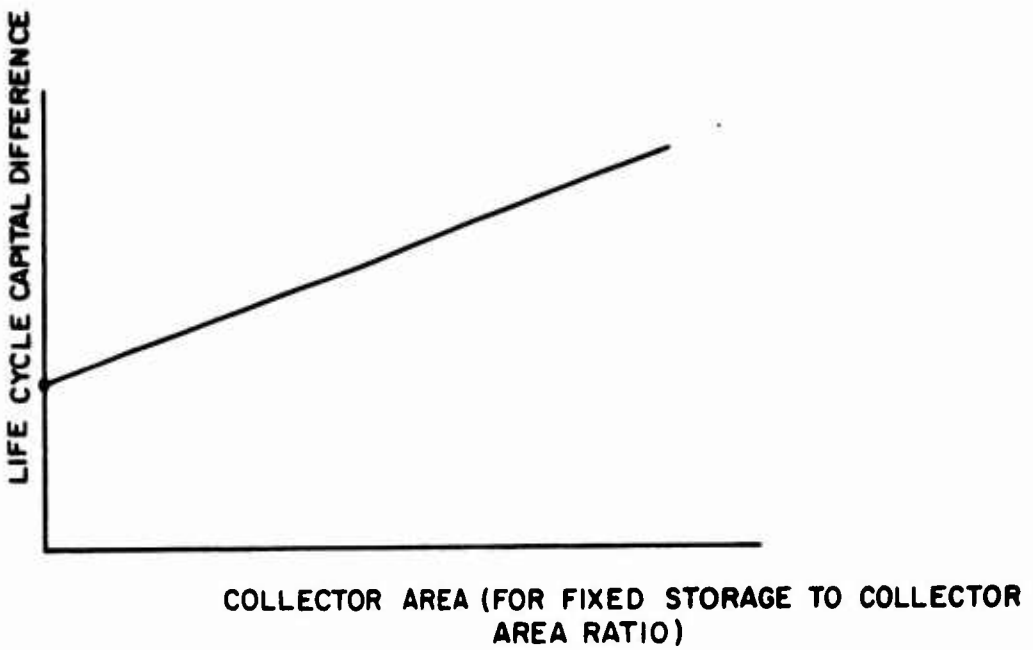

Figure 22. Life-cycle cost difference vs. collector area.

hours, and multiply by the local electrical rate to obtain the cost of cooling energy.

(3) Divide the input heat energy required for heating by the heating value of the fuel used, and multiply by the unit fuel price to determine the cost of heating.

(4) Add the results of (2) and (3) to obtain the total annual fuel cost.

(5) Convert the annual fuel cost to life-cycle (present worth) cost.

The amount of auxiliary fuel or electrical energy required annually for heating and cooling can be determined for various solar energy system sizes by referring to the site and building-specific performance curves generated by methods outlined in Chapter 3, p 15. To simplify the economic analysis, it is generally assumed that all thermal energy requirements are met by a single fuel source (gas, oil, or electricity). The procedure for determining life-cycle costs for various solar energy systems is:

(1) Determine the total auxiliary annual energy requirements for a given system, Q_c, by multiplying the total energy requirements, Q_L, by the fraction of the total requirements *not* met by solar energy, i.e., $Q_c = Q_L (1 - \rho)$.

(2) Determine annual energy cost by dividing the annual energy requirements by the heating value of the fuel, and multiplying this figure by the appropriate unit fuel price.

(3) Convert annual fuel cost to life-cycle (present worth) cost.

Figure 23 is a hypothetical plot of life-cycle fuel costs versus collector area generated by repeating steps 1 through 3 for different collector areas.

The total life-cycle cost difference between conventional and solar heating and cooling systems can now

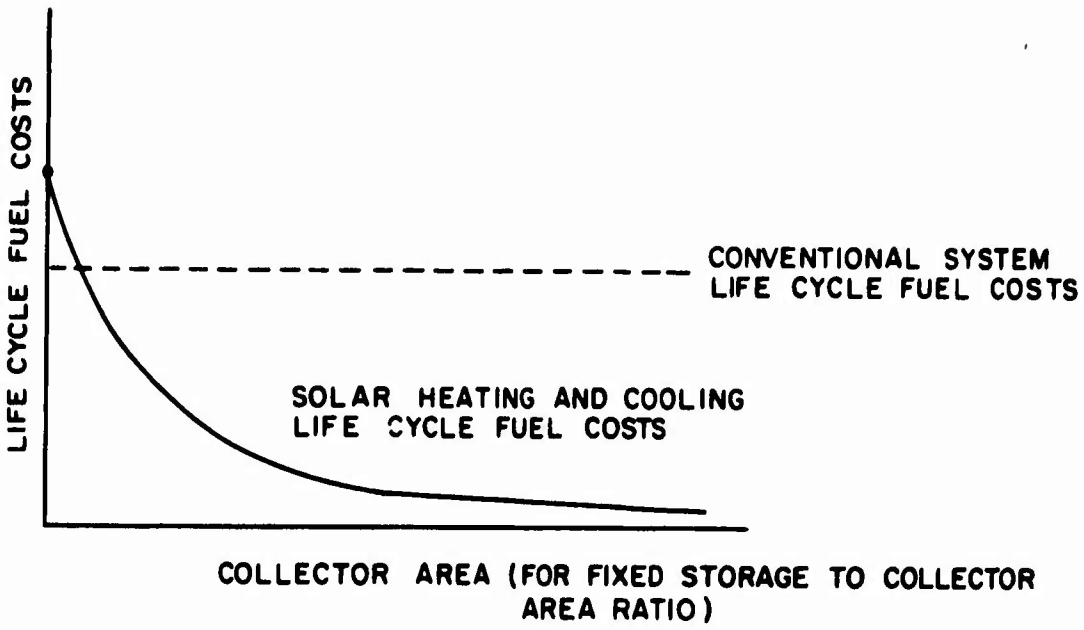

Figure 23. Life-cycle fuel costs vs. collector area.

be determined for various collector areas. For a given collector area, this difference is simply the life-cycle capital cost difference of the solar energy system (Figure 22) plus the life-cycle fuel cost for the same system (Figure 23) minus the life-cycle fuel cost of a conventional system. Figure 24 is a hypothetical plot of this cost difference for varying collector areas.

When the cost difference for the solar energy system being considered has been plotted (as in the form of Figure 24), the optimum collector area becomes obvious. To determine the optimum solar energy system, separate building and site-specific curves should be drawn for various collector types and storage-mass-to-collector area ratios. Note that Figure 24 concisely summarizes the economic feasibility of solar heating and cooling systems. The points on the curve having a positive cost difference indicate that solar energy is not cost-effective. Only when the curve dips below the origin can a solar energy system be economically justified. Based on present solar energy system costs, many applications may not have such a negative cost difference.

5 CONCLUSIONS AND RECOMMENDATIONS

Conclusions

Solar energy can meet much of the heating and cooling loads of Army buildings at most locations within the United States, and thus can potentially lower a facility's demand for conventional fuels significantly. Technically feasible solar energy systems can be installed at Army facilities with currently available commercial components.

The economic viability of solar energy systems varies greatly with location and building structure; thus, each application must be analyzed individually. Study results indicate that the single dimensionless curves shown in Chapter 3 are reasonable approximations of solar heating and cooling system performances for all buildings and sites studied. Therefore, for feasibility analysis, solar system performance can be estimated without using computer-aided techniques.

The methods described herein will provide a first estimate of economic feasibility; if this first estimate is promising, a more specific and detailed study can provide more precise design information.

An unavoidable conclusion, however, is that the *design* of solar energy heating and cooling systems is too complex for handbook methods; computer simulations of the form presented in this report are therefore required to obtain adequate design solutions.

Recommendations

It is recommended that solar energy be considered not as a panacea, but as one of many viable energy conservation alternatives which must be applied collectively to reduce the Army's and the nation's wasteful use of dwindling energy resources.

It is recommended that the method described herein be field-tested at a Corps District Office to validate its ease of use and applicability to designers. It is also recommended that the information and methods described in this report be applied to all new construction and to most existing well-insulated buildings to determine the economic feasibility of using solar energy for heating and cooling.

When comparing various types or brands of solar collectors, the procedures described in the NBS publication, *Methods of Testing for Rating Solar Collectors Based on Thermal Performance*[5] should be applied whenever the manufacturer's performance claims are in question.

Solar heating and cooling systems should generally be subject to the same reliability standards as conventional heating and cooling systems. The NBS publication, *Interim Performance Criteria for Solar Heating and Cooling Systems and Dwellings*,[6] provides additional information.

The Energy Research and Development Administration, in cooperation with the Department of Housing and Urban Development, has prepared a directory of manufacturers of solar heating and cooling system components,[7] which may be used as a source for current solar energy system component cost data.

[5] J. S. Hill and T. Kusuda, *Methods of Testing for Rating Solar Collectors Based on Thermal Performance*, NBSIR-74-635 (Thermal Engineering Systems Section, Center for Building Technology, December 1974).

[6] *Interim Performance Criteria for Solar Heating and Cooling Systems and Dwellings* (National Bureau of Standards, January 1, 1975).

[7] *Catalog on Solar Energy Heating and Cooling Products* (ERDA, 1975). (Available from Technical Information Center, P.O. Box 62, Oak Ridge, TN 37830.)

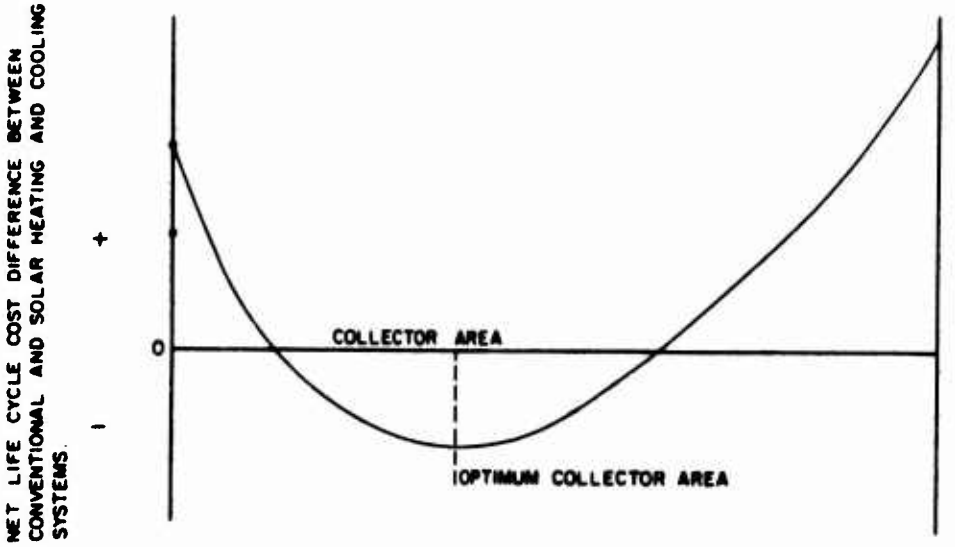

Figure 24. Net life-cycle cost difference vs. collector area.

APPENDIX A:

EXAMPLE OF ECONOMIC FEASIBILITY CALCULATIONS

The general approach to determining economic feasibility was described in Chapter 4, p 28. As an illustration, a specific building the headquarters and classroom at a specific site, Fort Hood, TX has been chosen arbitrarily. In order to make an economic assessment, an appropriate performance curve, $\rho(A_c)$, must be selected. Assuming that a storage capacity of 31 lb for each sq ft (151 kg/m^2) of collector is reasonable for the first estimate, we find from Figure 20 that

$$\rho = 0.309\,(r - 0.082\,r^2).$$

The parameter, r, depends on the annual energy requirements, Q_L, of the building and the radiation density, H_θ. Since it is to be expected that climatic conditions at Fort Hood are quite similar to those at Fort Worth, the Fort Worth value from Table 2, $Q_L = 1.23 \times 10^9$ Btu, can be used. From the solar radiation map (Figure 21), a daily horizontal radiation of 440 Langleys, and a latitude, θ_L, of 32° is estimated. To obtain the annual horizontal radiation density, H_θ, the daily value in Langleys is multiplied by 1.34×10^5 Btu/sq ft. The value for H_θ is then

$$H_\theta = \frac{H_o}{\cos(\theta_L - 8)} = 6.46 \times 10^5 \text{ Btu/sq ft.}$$

This leads to $r = H_\theta A_c / Q_L = 5.25 \times 10^{-4} \times A_c$. Substituting this into the equation for ρ gives the performance curve,

$$\rho = 1.62 \times 10^{-4}(A_c - 4.3 \times 10^5 A_c^2) \qquad \text{(Eq A1)}$$

which will be used in the following cost analysis.

Before examining the costs involved, some discussion of the cost data included in this example is required. Cost figures for capital equipment were generally obtained from equipment manufacturers. Other cost data, such as controls, piping, and labor, were based on the authors' experience and the use of standard estimating guides. Obviously, these cost figures will vary with location, manufacturer, and time; thus, although these figures are presently representative, they should not be taken as guidelines for economic studies. In addition, since this was an example to demonstrate the *method* of performing the economic analysis, no attempt was made to obtain hard economic data; standard textbook present-worth costing methods were used. Other life-cycle costing methods, such as described in *OCE Life Cycle Costing Instructions*, with amendments[8] can also be applied without changing the method of cost comparison. With this in mind, the example economic analysis can be made. Capital costs will be considered first.

Capital Costs

Of interest here is not the absolute cost of the components of the solar installation but the cost relative to those of a conventional system. Table A1 summarizes the estimated relative costs. An explanatory discussion follows.

The values in the table are estimates based on limited data. The net cost for auxiliary heating is zero, because it is sized to meet the peak load, the same as in a conventional system.

[8] *OCE Life Cycle Costing Instructions* (Department of the Army, May 1971).

Table A1

Capital Costs (CC) in Dollars

Component	Cost for Given Load	Cost/sq ft of Collector Area
Auxiliary Heating system	0	
Cooling System	1548	
Controls	3000	
Heat Exchanger		0.50
Collector Fluid		0.18
Storage Tank		1.00
Plumbing		0.75
Pumps		0.75
Collectors		5.00 or 10.00
Labor		1.00

Total $CC_1 = 4548 + 9.93 \times A_c$ for less expensive collector or
$CC_2 = 4548 + 14.93 \times A_c$ for more expensive collector

For the cooling system the cost of the solar absorption cooler (including cooling tower) is compared to a conventional, electrically driven reciprocating compression air conditioner. The peak cooling load (see Table 2) is 4.3×10^5 Btu/hr or about 36 tons for the Fort Hood building. Estimated costs are $460/ton for the gas absorption unit and $417/ton for the compression unit. This is a differential cost of $43/ton or $1548 for the 36 tons.

The cost of control sensors and valves is nearly independent of system size and is roughly estimated at $3000.

The rest of the items in the table are dependent on the collector area. Although not strictly true, it is assumed that the dependency is linear. Two values for unit collector costs are used; the higher value represents present low-volume production cost, and the lower value represents a possible future high-volume production cost.

Fuel Costs

The present-worth cost of fuel for the solar installation (PWC_s) may be expressed in terms of the collector area A_c by

$$PWC_s = PWC_s|_{A_{c=0}} [1-\rho(A_c)] \qquad \text{(Eq A2)}$$

where ρ is the fraction of the total energy met by solar energy as expressed in Eq A1 above, and $PWC_s|_{A_{c=0}}$ is the present-worth cost of fuel with zero collector area.

The total annual energy requirement for the Fort Hood building (see Table 2) is 1.23×10^8 Btu. It is assumed that the auxiliary heat is supplied by gas at a current cost of $1/million Btu. (This was the June 1975 rate at Fort Hood.) Thus, for $A_c=0$, the annual fuel cost is $1230. Using a 20-yr life, an annual discount rate of 10 percent, and an annual fuel escalation rate of 20 percent, then $PWC|_{A_{c=0}}$ =$68,900 and PWC=68,900 $[1-\rho]$.

Consider now the present worth of the fuel for the conventional system (PWC_c). Table 2 shows that the annual cooling load is 7.7×10^8 Btu. If the coefficient of performance (COP) is 3, the annual electrical consumption is 7.52×10^4 kWh. At $0.017/kWh, the annual cooling cost is $1278. Table 2 shows that the annual heating load is 4×10^7 Btu. At $1/million Btu for gas, the annual heating cost is $40. For heating and cooling the annual fuel cost is $40 + $1278 = $1318. For this cost and the same values for discount rate, life, and escalation rate, it can be seen that PWC_c = $76,216.

The net-present worth of fuel (PWC) is the difference of:

$$PWC = PWC_s \quad PWC_c = 68{,}900\ [1-\rho] \quad 76{,}216$$
$$= \quad 7316 \quad 68{,}900 \times \rho.$$

This may be expressed in terms of collector area by using Eq A1.

$$PWC = \quad 7316 \quad 68{,}900 \times 162$$
$$\times 10^{-4} (A_c \quad 4.3 \times 10^{-5} A_c^2)$$
$$= \quad 7316 - 11.2 \times A_c + 4.8 \times 10^{-4} \times A_c^2.$$

The net life cycle cost differential (LCC) is simply the sum of the capital cost and the present worth of fuel, i.e.,

$$LCC_1 = CC_1 + PWC$$
$$= 4548 + 9.93 \times A_c \quad 7316 - 11.2$$
$$\times A_c + 4.8 \times 10^{-4} A_c^2$$
$$= -2768 - 1.27 \times A_c + 4.8 \times 10^{-4} A_c^2$$

for the less expensive collector ($5/sq ft),

and

$$LCC_2 = -2768 + 3.73 \times A_c = 4.8 \times 10^{-4} A_c^2$$

for the more expensive collector ($10/sq ft).

These two life-cycle costs are plotted in Figure A1. It shows that for the less expensive collector, the solar installation is cheaper than the conventional installation up to a collector area of 4100 sq ft (377 m^2). The savings, although modest, are greatest for a collector area of about 1500 sq ft (138 m^2). The more expensive collector causes the solar system to cost more, although the added cost is small compared to the total life-cycle cost of the system.

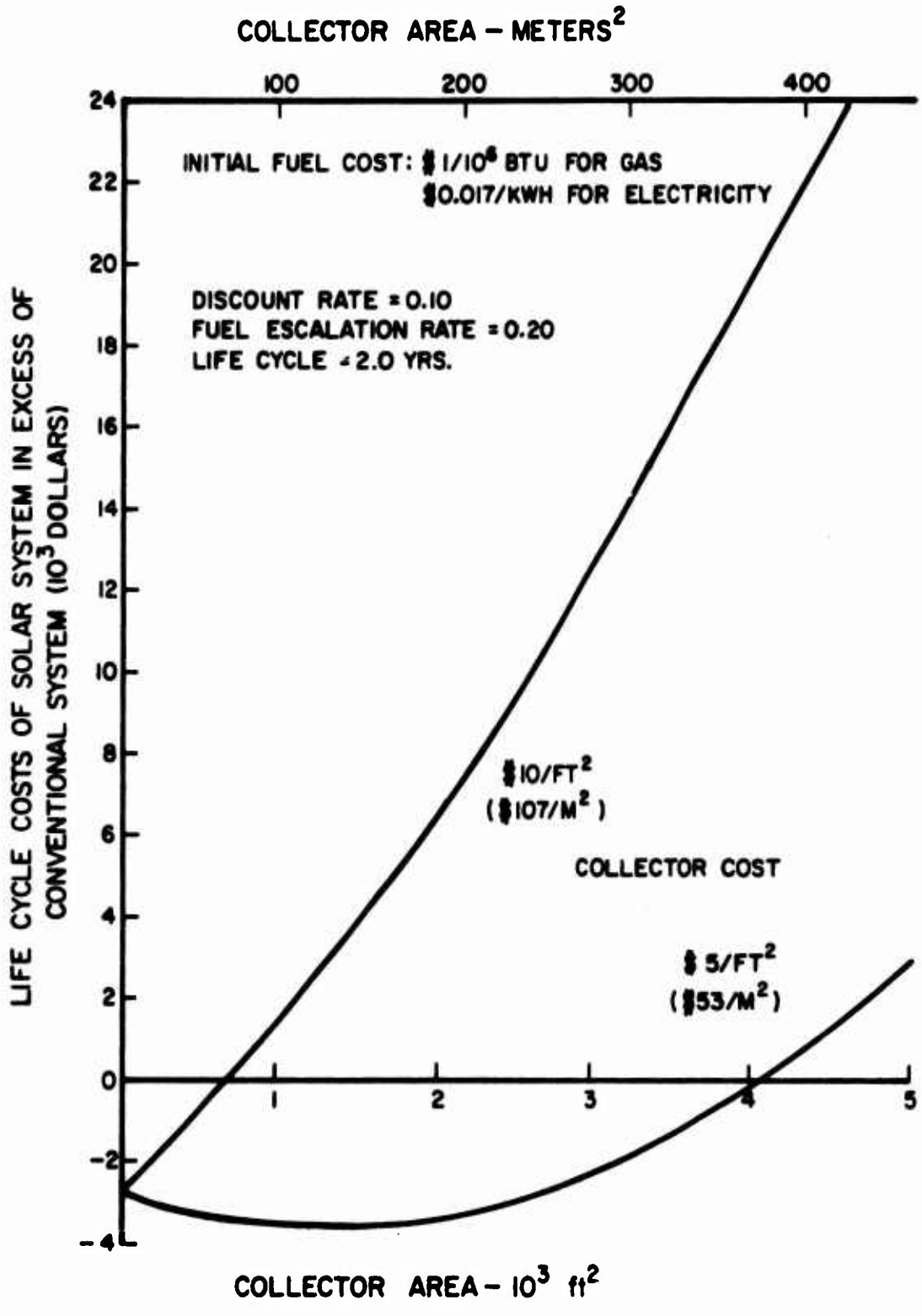

Figure A1. Example of life-cycle costs for HQ building at Fort Hood, TX.

APPENDIX B:
NBSLD—BRIEF PROGRAM DESCRIPTION

The hourly heating and cooling load for each building at each site was estimated by using a modified version of the National Bureau of Standards Load Determining Computer Program (NBSLD). This program uses the thermal response factor method to estimate conduction and thermal capacitance of walls, floors, and roofs, and performs a detailed hourly heat balance on all interior surfaces. The program permits consideration of variable internal space temperatures and provides full consideration of the effects of window and wall shading; internal occupancy, lighting, and equipment loads; building use schedules, infiltration and ventilation air loads; and building orientation.

Both buildings studied in this report were simulated as single zones. The building's long axis was assumed to be east-west oriented; the building was assumed to be heated when space temperature was 68°F (25.3°C) or above. Construction details and lighting loads were obtained from construction drawings of the buildings. Occupancy and lighting schedules were estimated from available historical data and information obtained from users of identical existing facilities.

The NBSLD program was used because it is recognized as one of the most precise load-predicting programs available. This precision was particularly important to follow-up solar simulation studies because of the hourly building thermal load's critical impact on estimating overall performance of solar heating and cooling systems.

APPENDIX C:
SOLAR HEATING AND COOLING SYSTEM SIMULATION PROGRAM DESCRIPTION

Introduction

To perform this study, it was necessary to develop an efficient program for parametric analysis of solar heating and cooling systems. Year-long, hour-by-hour system operation simulations were necessary to account for daily and seasonal variations of heating and cooling loads and for the availability of sunlight. In order to save computing time, the computer program, SOLSYS, was developed with a single subroutine, rather than several, to describe the entire solar heating and cooling system. The greatest time savings resulted from segmentation of the program and subroutine, so that numbers unchanged from the previous hour or iteration were not recalculated. The data input method was written so that many runs could be made sequentially, with only one or a few parameters changed for each run.

System Description

Figure C1 is a diagram of the simulated solar heating and cooling system. The heart of the system is the storage tank, which stores energy in a liquid (probably water with suitable corrosion inhibitors) in the form of sensible heat. The solar collectors are separated from the storage tank by a heat exchanger. This allows use of an expansive fluid in the collectors which will not freeze or boil when the collector pump is not operating.

The heater is a simple heat exchanger mounted in the air duct. The air conditioner is a lithium bromide-water absorption air conditioner. It was modeled by a least squares fit to performance curves on a graph, showing capacity versus generator inlet temperature and outdoor wet bulb temperature for an ARKLA 3-ton unit.[9] If the storage tank temperature is too low to operate the air conditioner or to provide sufficient heating, the bypass valve diverts flow through the auxiliary heater, which heats the water to designated temperatures for heating or cooling.

All heat losses, both from piping and from addition of heat to the fluids caused by pump inefficiencies, were ignored. Heating and cooling loads were calculated separately. The NBSLD program[10] was used to create a data tape for SOLSYS, which provided hourly values of sensible heating or cooling load, latent cooling load, dry bulb temperature, wet bulb temperature, wind speed, and total solar radiation incident on a horizontal surface.

Program Description

SOLSYS is comprised of the main program, the system subroutine, and several small subroutines. The main program controls the data reading, iteration, and print processes. Subroutine SYSTEM is the system

[9]Correspondence from Dr. Philip Anderson to Doug Hittle (CERL); Subject: ARKLA Cooler, February 27, 1974.

[10]*NBSLD, Computer Program for Heating and Cooling Loads in Buildings* (National Bureau of Standards, 1974).

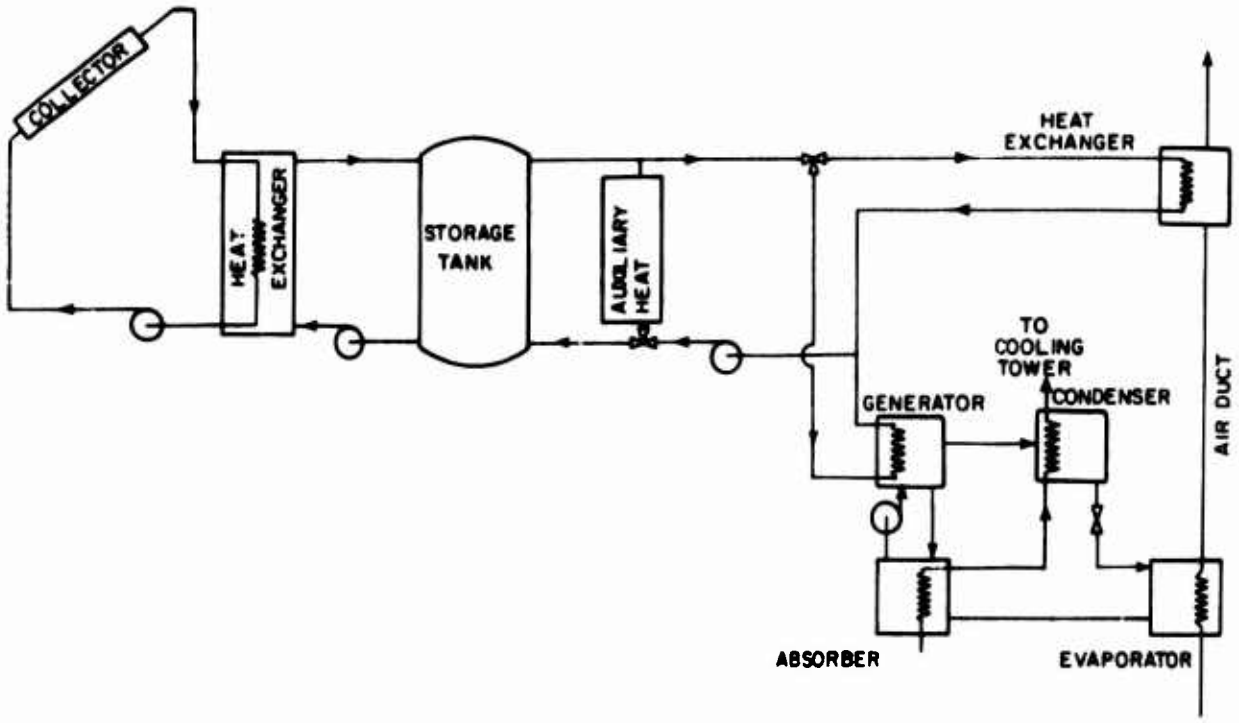

Figure C1. Diagram of simulated heating and cooling system.

model. Subroutines PRNT1, PRNT2, PRNT3, and PRNT4 print various outputs called from SOLSYS. Subroutines AC3T and TRNSAB, which are called from SYSTEM, are polynomial expressions for absorption air conditioner performance and the transmittance-absorptance product for the collector cover.

Figure C2 is a block diagram of the main program, which is comprised primarily of an initialization section and a cyclic section.

The initialization section first reads the data cards which select the outputs to be printed and provide output column headings. The section then reads a $CONTROL card, which uses namelist input[11] to designate the variable values which control program execution. A check is then made on one of the control variables which continues or terminates the program. Next, the initial values of the load and weather data and the initial storage tank temperature are read from an $INITIAL card. Then the initialization section of the SYSTEM subroutine is called, which reads parameters describing the system from the $PARAM card and computes any values which are constant throughout the simulation.

Next the program checks the control variable which specifies that an instantaneous performance calculation or a dynamic simulation will be performed. For a single, instantaneous calculation, the SYSTEM subroutine is called, and the desired outputs are printed. The program returns to point A, where new control variables, initial values, or system parameters may be read.

For the dynamic run, initial values are set for all indexing parameters, and the data tape is positioned to read the first day's data. The tape reader section has been written for a specific tape format and would have to be altered if a different format were used.

Control then transfers to point B in the cyclic section. The cyclic section also has a tape reader to read a new day of data when required. This tape-reading section includes an end-of-file check to terminate simulation, in addition to an end-of-run check against one of the control variables.

[11] *FORTRAN Extended, Version 4, Reference Manual* (Control Data Corporation, 1974).

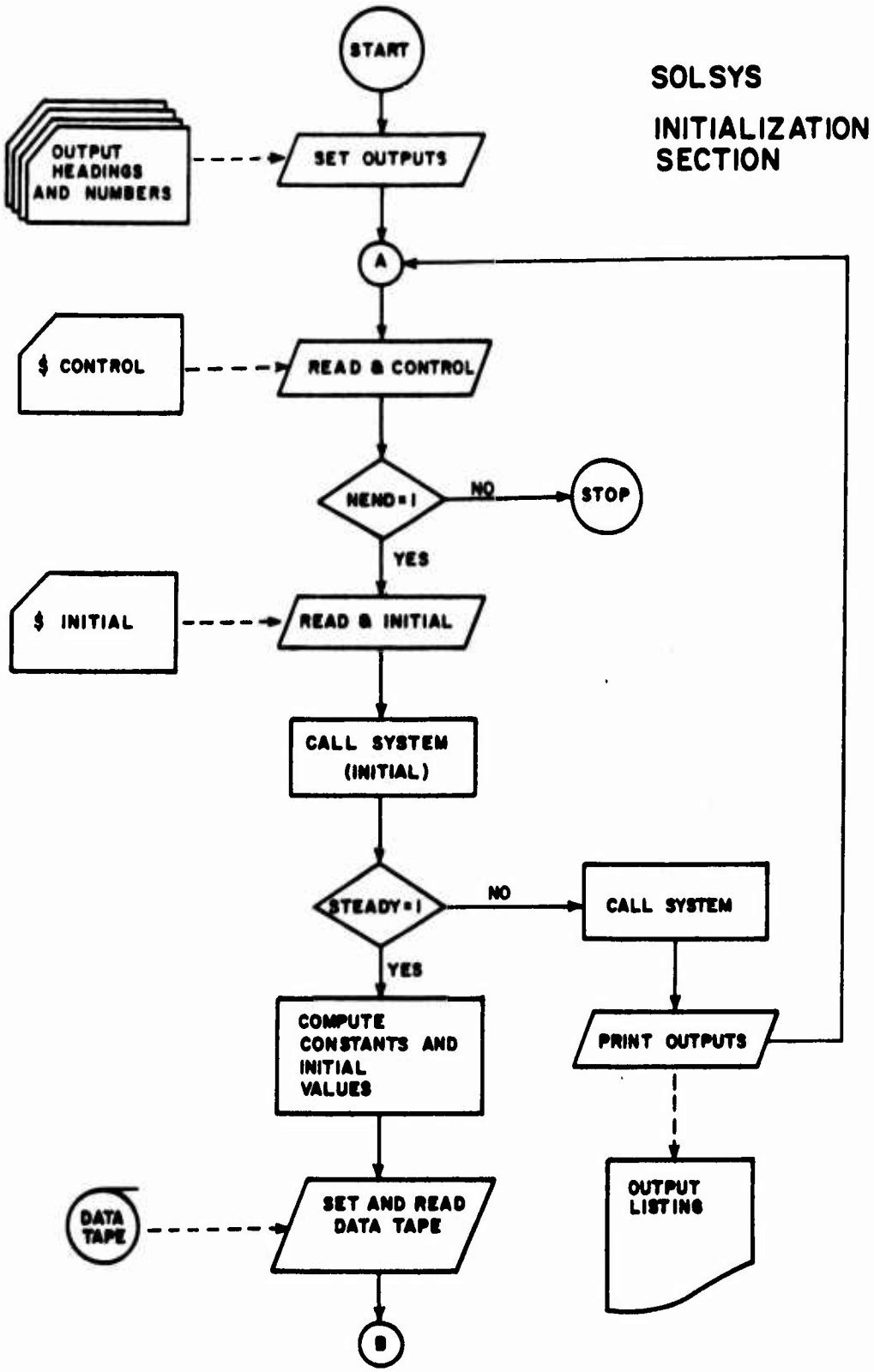

Figure C2. SOLSYS main program.

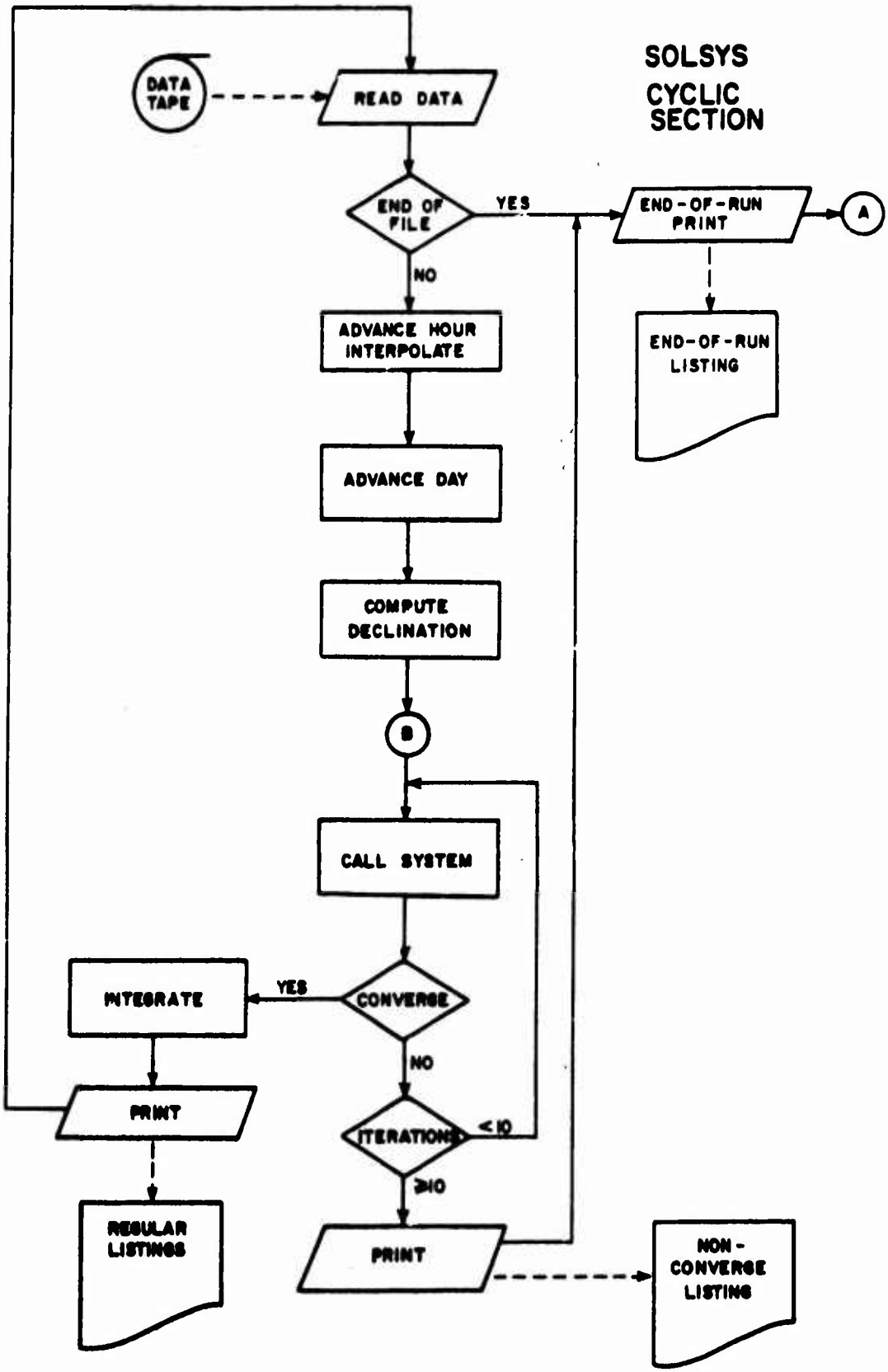

Figure C2. (cont'd).

The hour record is then advanced by one time step. A linear interpolator is available if the time step is less than the time between data points on the tape, which must be an integral multiple of the time step. Also, it should not be less than the time step, since some data would then be ignored.

The day record is advanced when hour 24 is reached, and the solar declination for that day is calculated. Point B (entry from the initialization section) is just after the declination calculation.

Next, the iteration section computes the end of time step tank energy from the beginning, and the SYSTEM subroutine calculates the system performance. Iteration is terminated when the relative error between two successive iterations is sufficiently small. There is also an iteration counter which will terminate iteration and the current simulation by printing the data array for the day, the current values of the output array, and the values of the tank energy for each iteration in the current time step. These values can be helpful for determining the reason for nonconvergence. Control then goes to point A for the next simulation.

Converged iterations pass to the integration section, where certain outputs, such as total solar energy collected, are integrated over time by means of a simple, trapezoidal numerical integrator.

Then the outputs are printed according to the two print control variables. One specifies whether every time step will be printed; the other specifies the occurrence of printing once per day at midnight. The daily printer gives daily integrated values for all integrable outputs. The program then returns to the tape reader section to begin the next time step.

After reaching the end of the simulation, a terminal printout is made which includes outputs integrated over the entire run. Control then passes to point A in the initialization section to begin a new simulation. Here, the value of namelist input appears; the namelist cards ($CONTROL, $INITIAL, $PARAM) contain only variables whose values differ from those of the previous simulation. All unlisted variables remain unchanged.

Figure C3 is a diagram of the SYSTEM subroutine, which is composed of three main sections: initialization, control, and performance.

The initialization section is entered only at the beginning of each simulation. It reads and prints the system parameters and calculates all values which will not change during a dynamic simulation. The control section is entered only at the beginning of each time step. It determines the mode of operation of each system component and calculates all values which are constant during the time step.

The performance section, which calculates the performance of each system component based on the mode of operation, is entered during every iteration. Each system component is a separately written section having certain parameters, inputs, and outputs. These sections are connected within the subroutine by equivalence statements. The following sections provide operational details of various parts of the program.

Convergence

The iterative process is based on computing end-of-time-step tank energy (E_e), which is based on beginning-of-time-step energy (E_0) and the change in energy caused by system operation. The system subroutine computes rate of energy change ($F = dE/dt$) based on the average tank energy during the time step ($E_{avg} = [E_0 + E_e]/2$). For the first iteration, it is assumed that $E_0 = E_{avg}$. A first estimate for end-of-time-step energy (E_1) is calculated from $E_1 = E_0 + F\Delta t$. In the second iteration, the system subroutine uses $E_{avg} = (E_0 + E_1)/2$ to compute a new F, which is used to compute a new end-of-time-step energy (E_2).

This iterative process terminates when the relative error between two successive end-of-time-step energies is less than the specified convergence limit (e).

$$2\left|\frac{E_n - E_{n-1}}{E_n + E_{n-1}}\right| < e$$

The significance of the convergence limit is more apparent when the tank energy is specified in terms of its temperature, $E = mc_pT$.

T_{avg}	e	Maximum value of $T_n - T_{n-1}$ which satisfies convergence
100 F	.1	10°F (−12.1°C)
200 F	.1	20°F (−6.6°C)
100 F	.01	1°F (−17°C)
200 F	.01	2°F (−16.5°C)

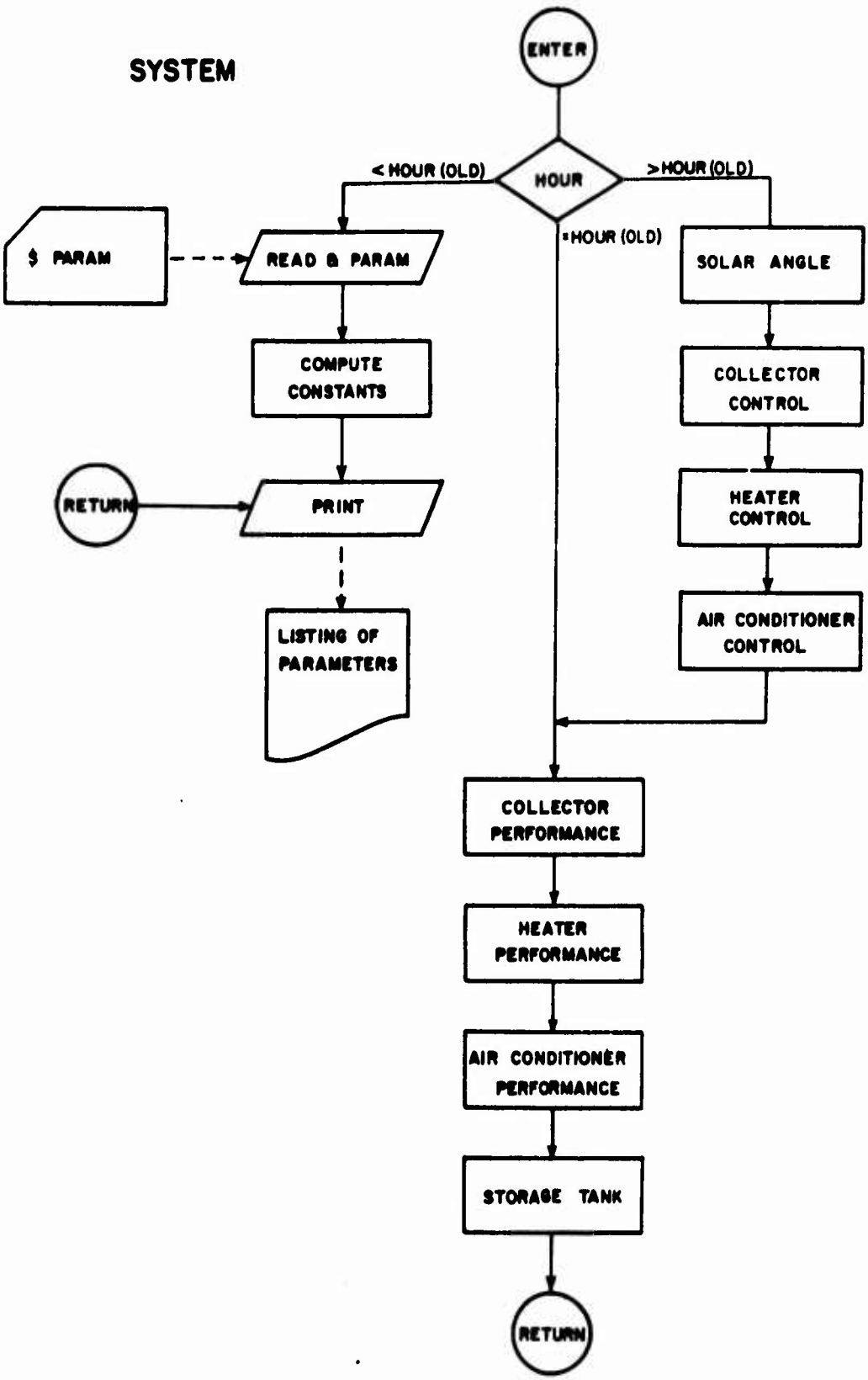

Figure C3. SYSTEM subroutine.

If the relationship between tank size and change in energy is such that the tank temperature cannot change by the amount in the third column, there will be no second iteration, and the solution will appear to converge. On the other hand, very small values for the convergence limit are unnecessary, because system inputs are relatively cyclic, and errors in one portion of the cycle tend to be canceled by errors in another portion. A limit of ten iterations was allowed for occurrence of convergence.

Two convergence problems were encountered during the development of this program. The first was the switching between operating modes in the SYSTEM subroutine, and the second was the model's inherent instability when small storage tanks were used.

For example, when the heater is operational it will pump energy from the tank, thereby reducing the tank temperature, as long as the tank temperature is above some specified value. When tank temperature is below this specified value, the pumping stops and the following situation may occur. At the beginning of the time step, the tank temperature is just above the cut-off value. Energy is removed from the tank during the first iteration; however, during the second iteration, the average tank temperature is below the cut-off value, so the pump will not operate. E_2 then will equal E_0, since no energy was removed from the tank during the second iteration. The third iteration will now be exactly the same as the first, and the fourth will be the same as the second, etc. The collector and air conditioner have similar operational cut-off points.

This problem was handled by splitting the SYSTEM subroutine into control and performance sections. The control section determines the mode of operation one time, and determines whether water for the heater is being pumped from storage. The performance section, which is entered at every time step, cannot change the mode of operation. This technique is inaccurate to the extent that the tank temperature can change during one time step, and is thus less accurate for smaller tanks; however, the cyclic nature of the dynamic problem causes error cancellation over a long time period.

When small storage tanks were used, several cases of nonconvergence were observed where successive iterations oscillated around an apparent convergence point (See Figure C4). The convergence was too slow for the convergence criterion to be met in ten iterations.

By defining $\Delta 1 = E_1 - E_0$

$\Delta 2 = E_2 - E_1$

$\Delta 3 = E_3 - E_2$

•

•

•

It was observed that $\Delta 1/\Delta 2 \cong \Delta 2/\Delta 3 \cong \Delta 3/\Delta 4 \ldots$

Assuming $\Delta 1/\Delta 2 = \Delta 2/\Delta 3 = \Delta 3/\Delta 4 = \ldots = R$, it can be shown that

$$E_e = E_2 - \frac{E_2 - E_1}{1 - R} \qquad \text{(Eq C1)}$$

This method successfully extended the lower limit of tank size to about one-half of its original value. Further tank size reduction led to divergence, so the assumption of constant ratios was no longer valid; however, convergence could still be achieved by reducing the time step size.

It was considered desirable to use the longest time step possible to minimize iterations for a 1-yr run. Nonconvergence with the corrector occurred when

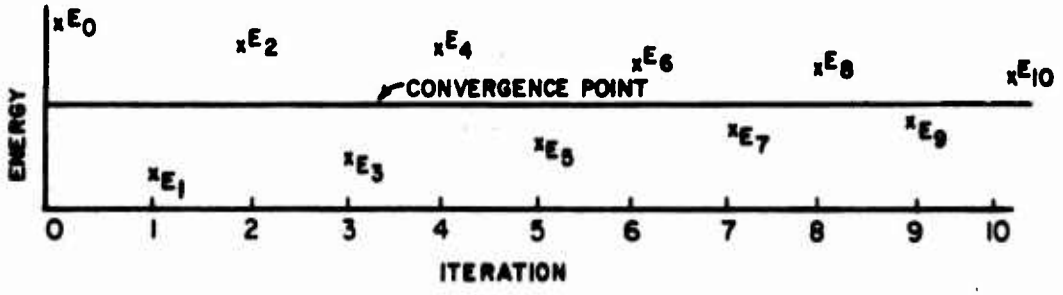

Figure C4. Energy vs. number of iterations for slowly converging case.

tank size was so small that a 20-degree change in tank temperature occurred at maximum load. Such an extreme change contradicts the quasisteady assumption used to derive the system performance equations. Therefore, it is probably not desirable to pursue additional means of achieving convergence without reducing the time step.

Solar Radiation Equations

Solar radiation is input as the intensity (Btu/hr/sq ft) on a horizontal surface. This figure must be converted into components of beam, diffuse, and reflected radiation, so that collector performance can be calculated. This was done by following the technique presented by ASHRAE and used in NBSLD.[12]

ASHRAE gives the intensity of beam radiation as

$$I_b = A\, e^{(-B/\sin\beta)} \qquad \text{(Eq C2)}$$

where A = apparent solar irradiation at air mass = 0
B = atmospheric extinction coefficient
β = solar altitude

The diffuse radiation on a horizontal surface is given by

$$I_d = C\, I_b \qquad \text{(Eq C3)}$$

where C = diffuse radiation factor

NBSLD modifies these two equations to

$$I_b' = DAe^{(-B/\sin\beta)}$$

and

$$I_d' = CI_b'/D^2$$

where D = atmospheric clearness number[13]

From these two equations, the intensity of radiation on a horizontal surface is

$$I_h = I_b' \sin\beta + I_d' = I_b' \sin\beta + CI_b'/D^2 \qquad \text{(Eq C4)}$$

Therefore, $I_b' = I_h/(\sin\beta + C/D^2)$. (Eq C5)

The angle of beam radiation incidence on a tilted surface is given by

$$\cos\theta_c = \sin\delta \sin\phi \cos s - \sin\delta \cos\phi \sin s \cos\gamma + \cos\delta \sin\phi \cos s \cos\omega + \cos\delta \sin\phi \sin s \cos\gamma \cos\omega + \cos\delta \sin s \sin\gamma \sin\omega \qquad \text{(Eq C6)}$$

where

ϕ = latitude of site (north positive)

δ = solar declination

s = slope of the surface

γ = azimuth of the surface (south = 0, east = +)

ω = hour angle

The angle of incidence on a horizontal surface is given by

$$\cos\theta_h = \sin\delta \sin\phi + \cos\delta \cos\phi \cos\omega \qquad \text{(Eq C7)}$$

Note that $\cos\theta_h = \sin\beta$.

The view factor between the collector and the sky is $F_{cs} = (1 + \cos s)/2$. The view factor between the collector and the ground if $F_{cg} = (1 - \cos s)/2$.

The total radiation incident on the collector is

I_t = beam radiation + diffuse radiation + reflected radiation

$$= I_b' \cos\theta_c + I_d' F_{cs} + (I_b' \cos\theta_h + I_d')\, \rho_g F_{cg} \qquad \text{(Eq C8)}$$

where ρ_g = reflectivity of the ground.

To avoid recalculation of the sine and cosine terms, the radiation calculations appear in several parts of the program. Since latitude, slope, and azimuth will not change during a simulation, they are calculated once in the initialization section of SYSTEM. Declination and the diffuse radiation factor are computed once daily in the main program. Angle and radiation intensity are computed once hourly for each time step.

[12] *ASHRAE Handbook of Fundamentals* (American Society of Heating, Refrigerating, and Air Conditioning Engineers, Inc., 1972), p 394.

[13] J. A. Duffie and W. A. Beckman, *Solar Energy Thermal Processes* (John Wiley and Sons, 1974), p 15.

Collector Equations

Figure C5 illustrates the system configuration and variables used in the collector equations.

Parameters:

A	collector area
$(\tau\alpha)$	transmittance-absorptance product
c_{pc}	specific heat of collector fluid
$\dot{m}_c$	mass flow rate of collector fluid
F'	collector geometry efficiency factor[14]
U_{be}	edge and back heat loss coefficient
N	number of glass covers
ϵ_p	collector plate emissivity
E	heat exchanger effectiveness
c_{pt}	specific heat of tank fluid
$\dot{m}_t$	mass flow rate of tank fluid

Inputs:

S	solar radiation on the collector
T_a	ambient dry bulb temperature
w	wind speed
T_1	temperature of fluid from tank

Computed values:

$$\gamma = \frac{\dot{m}_c C_{pc}}{U_L A}$$

$$C_c = \dot{m}_c C_{pc} \qquad F_r = \gamma\left(1 - e^{\frac{F'}{\gamma}}\right)$$

$$C_t = \dot{m}_t C_{pt} \qquad \alpha = \frac{AF_r U_L}{C_c}$$

$$C_{min} = \text{min of } \frac{C_c}{C_t} \qquad \beta = \frac{EC_{min}}{C_c}$$

The rate of energy collection, q_u, can be expressed by the following formula:[15]

$$q_u = AF_r[S(\tau\alpha) - U_L(T_4 - T_a)] \qquad \text{(Eq C9)}$$

Also, $q_u = \dot{m}_c c_p(T_2 - T_4)$ or $T_2 = T_4 + q_u/C_c$

(Eq C10)

The heat exchanger equation is

$$T_4 = \frac{EC_{min}(T_1 - T_2)}{C_c} + T_2 \qquad \text{(Eq C11)}$$

[14] R. W. Bliss, "The Derivation of Several Plate Efficiency Factors Useful in the Design of Flat-Plate Solar Heat Collectors," *Solar Energy*, Vol 3, No. 4 (1959), pp 55-64.

[15] J. A. Duffie and W. A. Beckman, *Solar Energy Thermal Processes* (John Wiley and Sons, 1974), p 241.

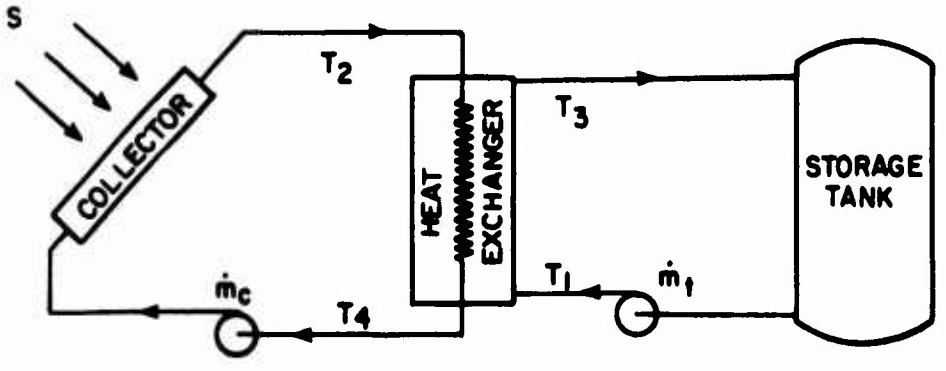

Figure C5. Collector-storage tank system schematic.

There are three unknowns (q_u, T_4, T_2) in these three equations. Substituting Eqs C10 and C11 into Eq C9 gives

$$T_2 = \frac{1}{C_c}\left\{F_r A[S(\tau\alpha) \quad U_L(\frac{EC_{min}(T_1 \quad T_2)}{C_c} + T_2 \quad T_a)]\right\} + \frac{EC_{min}(T_1 \quad T_2)}{C_c} + T_2$$

$$T_2 = \frac{F_r AS(\tau\alpha)}{C_c} \quad \frac{F_r AU_L EC_{min} T_1}{C_c^2} + \frac{F_r AU_L EC_{min} T_2}{C_c^2} \quad \frac{F_r AU_L T_2}{C_c} + \frac{F_r AU_L T_a}{C_c} + \frac{EC_{min} T_1}{C_c} \quad \frac{EC_{min} T_2}{C_c} + T_2$$

$$T_2 = \frac{\alpha S(\tau\alpha)}{U_L} \quad \alpha\beta T_1 + \alpha\beta T_2 \quad \alpha T_2 + \alpha T_a + \beta T_1 \quad \beta T_2 + T_2$$

$$T_2 = \frac{\frac{\alpha S(\tau\alpha)}{U_L} + (\beta - \alpha\beta)T_1 + \alpha T_a}{\alpha + \beta - \alpha\beta} \qquad \text{(Eq C12)}$$

The other unknowns can now be found.

$$q_u = EC_{min}(T_2 - T_1)$$

$$T_4 = T_2 - q_u/C_c$$

$$T_3 = T_1 + q_u/C_t$$

The overall heat loss coefficient, U_L, is a function of collector construction and operating conditions. The following expression was developed by S. A. Klein[16] from experimental studies.

$$U_L = \frac{3.6}{\frac{N}{\frac{C}{T}\left[\frac{(T \quad T)}{N+f}\right]^{.33}} + \frac{1}{h_w}} + \frac{(T_p+T_a)(T_p+T_a)}{\frac{1}{\epsilon_p + .05N(1 \quad \epsilon_p)} + \frac{2N + f \quad 1}{\epsilon_p} \quad N} + U_{be}$$

(Eq C13)

$[KJ\ hr^{-1}\ m^{-2}\ K^{-1}]$

where

T_p = mean collector plate temperature

$= (T_2 + T_4)/2$

$h_w = 20.52 + 13.68\ w$

$f = (1 \quad .04h_w + .0005h_w^2)(1 + .091N)$

$C = 365.9(1 \quad .00883s + .0001298s^2)$

s = collector slope (degrees)

Since U_L is a function of T_2 and T_4, its value is most conveniently found iteratively; however, since it is a weak function of T_2 and T_4, it is evaluated only on the first iteration in each timestep.

The transmittance-absorptance product is given by[17]

$$(\tau\alpha) = \frac{\tau\alpha}{1 - (1 \quad \alpha)\rho_d} \qquad \text{(Eq C14)}$$

where

α = collector plate absorptance

τ = cover transmittance $= \frac{1 - \rho}{1 + (2N \quad 1)\rho} \times e^{-KL}$

= τ due to reflection * τ due to absorption

$$\rho = \frac{1}{2}\left[\frac{\sin^2(\theta_2 - \theta_1)}{\sin^2(\theta_2 + \theta_1)} + \frac{\tan^2(\theta_2 - \theta_1)}{\tan^2(\theta_2 + \theta_1)}\right]$$

where θ_1 and θ_2 are as shown in Figure C6

[16] S. A. Klein, "Calculation of Flat-Plate Collector Loss Coefficients," paper presented at U. S. Section meeting, International Solar Energy Society, Fort Collins, CO (1974).

[17] J. A. Duffie and W. A. Beckman, *Solar Energy Thermal Processes* (John Wiley and Sons, 1974), p 111.

K = extinction coefficient

L = distance light travels through the cover.

To save computer time, a least squares fit was performed for 1, 2, and 3 cover systems and the results expressed as a sixth-order polynomial. The polynomial is accurate to within 1 percent for low iron glass.

The collector has two modes of operation: both pumps either may be pumping or not pumping. This model assumes pumping whenever the energy collected is positive. Actual operation would involve temperature sensors which would start the pumps whe.: $T_2 < T_1$.

Figure C6. Incident and refracted angles.

Heater Equations

The heater shown in Figure C7 is operated by either stored or auxiliary heat. Actual control of this heater would involve a dual deadband with three temperatures: $T_x > T_y > T_z$. When the room air temperature, T_a, falls below T_y, the pump starts; if T_a rises above T_x, the pump stops. But if T_a falls below T_z, the valve will divert the flow through the auxiliary heater, which will operate until $T_a > T_y$. The auxiliary heater operates by heating the water to a specified temperature, T_3. If the storage temperature is so low ($T_1 < T_{min}$) that it is inefficient to pump from the storage tank, the valve will always divert through the auxiliary heater.

Parameters:

$\dot{m}_c$ mass flow rate produced by pump

c_p fluid specific heat

EC_{min} heat exchanger effectiveness multiplied by minimum heat rate (heat rate of the air)

T_{min} minimum storage tank temperature

T_3 temperature from auxiliary heater

T_a room air temperature (treated as a constant)

Inputs:

T_1 tank temperature

q_{load} heating load

Outputs:

q_s heating load met from storage

q_a heating load met from auxiliary

T_2 temperature of fluid returning to storage tank

$\dot{m}$ average mass flow rate to and from storage

The equations describing this system are based on two maximum heating rates and the heat exchanger equation. The maximum rate of transferring heat from the storage tank to the room air is

$$(q_s)_{max} = EC_{min}(T_1 - T_a) = \dot{m}_c c_p (T_1 - T_2) \quad \text{(Eq C15)}$$

The maximum rate of transferring heat from the auxiliary heater is

$$(q_a)_{max} = EC_{min}(T_3 - T_a) = \dot{m}_c c_p (T_3 - T_2) \quad \text{(Eq C16)}$$

This heater has four modes of operation. First T_1 may be less than T_{min}; in this case, $\dot{m} = 0$, $q_s = 0$, and $q_a = q_{load}$. Note that $(q_a)_{max}$ must be greater than the maximum probable heating load. This, in combination with the auxiliary heater temperature, T_3, determines the size of the heat exchanger.

In the second mode, the entire heating load can be met by pumping from storage; that is, when $(q_s)_{max} > q_{load}$, then $q_s = q_{load}$ and $q_a = 0$. During a 1-hour period, the entire heating load can be met by pumping for only a fraction (Y) of the hour, where $Y = q_{load}/(q_s)_{max}$. Then the average flow rate for the stor-

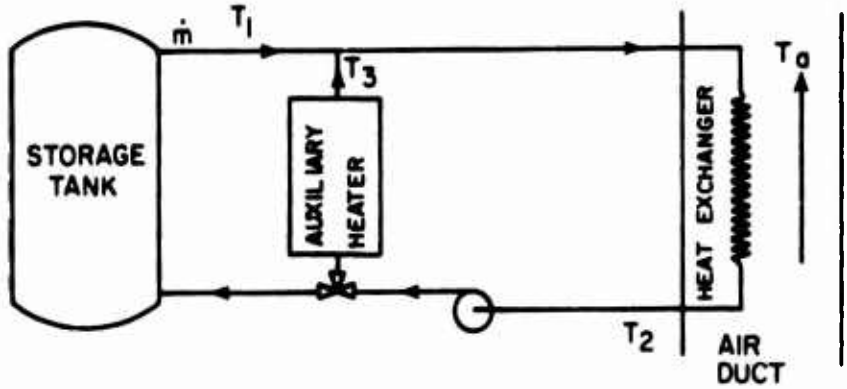

Figure C7. Auxiliary heater circuit.

age tank is $\dot{m} = Y\,\dot{m}_c$, and during pumping, $T_2 = T_1 - (q_s)_{max}/\dot{m}_c c_p$.

In the third operating mode, $(q_s)_{max} < q_{load}$. Sufficient heat must then be added from the auxiliary to meet the load. To make maximum use of stored energy, heat will be transferred from storage whenever the auxiliary is not operating. If Y is the fraction of each hour that heat is being transferred from storage, then,

$$q_{load} = Y\,(q_s)_{max} + (1-Y)(q_a)_{max} \qquad \text{(Eq C17)}$$

or

$$Y = \frac{q_{load} - (q_a)_{max}}{(q_s)_{max} - (q_a)_{max}}$$

The values of the outputs are $\dot{m} = Y\,\dot{m}_c$, $T_2 = T_1 - (q_s)_{max}/\dot{m}_c c_p$, $q_s = Y\,(q_s)_{max}$, and $q_a = (1-Y)(q_a)_{max}$.

Finally, in the fourth mode there may be no heating load. Then $\dot{m} = q_s = q_a = 0$.

In this analysis, the thermal capacity of the heater circuit fluid has been neglected. This should be a reasonable assumption if switching between auxiliary heating and storage heating occurs only a few times per hour, and there is relatively little piping between the auxiliary and the heat exchanger.

Absorption Air Conditioner Equations

An absorption air conditioner is especially attractive for solar energy cooling because it uses relatively low-temperature heat as its primary energy source. Solar air conditioning permits greater year-round use of solar collector and storage components. Absorption air conditioners currently in production have not been optimized to operate at temperatures produced by solar collectors. The following model is based on a 3-ton (36,000 Btu/hr) LiBr-water unit designed to operate using water at 210°F (93.2°C), but capable of using it at temperatures as low as 170°F (76.6°C) before crystallization occurs.

The air conditioning system shown in Figure C8 uses the same type of circuit as the heater, so its operating equations are similar.

Parameters:

$\dot{m}_c$	mass flow rate produced by pump
c_p	fluid specific heat
CAP	air conditioner capacity
COP	coefficient of performance
T_{min}	minimum generator inlet temperature
$(T_a)_{max}$	maximum ambient temperature for no cooling

Inputs:

T_1	storage tank temperature

q_{load}	cooling load
T_a	ambient dry bulb temperature
T_w	ambient wet bulb temperature

Outputs:

Q_s	energy from storage used for air conditioning
Q_a	energy from auxiliary used for air conditioning
T_2	temperature of fluid returning to storage tank
$\dot{m}$	average mass flow rate to and from storage.

The air conditioner absorber and condenser are cooled by a cooling tower. The air conditioner performance is expressed as a function of rated capacity, based on the generator inlet and outside wet bulb temperatures; therefore, the maximum cooling available by using stored energy is

$$(q_s)_{max} = CAP \cdot f(T_1, T_w)$$

and the maximum cooling rate using auxiliary energy is

$$(q_a)_{max} = CAP \cdot f(T_3, T_w)$$

The energy used to obtain a given amount of cooling is

$$Q = q/COP$$

There are four operating modes. In the first mode, $T_1 < T_{min}$. Then $m = 0$, $Q_s = 0$, and $Q_a = q_{load}/COP$.

In the second operating mode, the entire cooling load can be met from storage. $Q_s = q_{load}/COP$ and $Q_a = 0$. The fraction of each hour requiring pumping is $Y = q_{load}/(q_s)_{max}$. Thus,

$$\dot{m}c = Y\dot{m}_c \text{ and } T2 = T1 - \frac{(q_s)_{max}}{m_c c_p COP}.$$

In the third mode, $(q_s)_{max} < q_{load}$. Letting Y be the fraction of each hour that energy is removed from storage,

$$Y = \frac{q_{load} - (q_a)_{max}}{(q_s)_{max} - (q)_{max}}$$

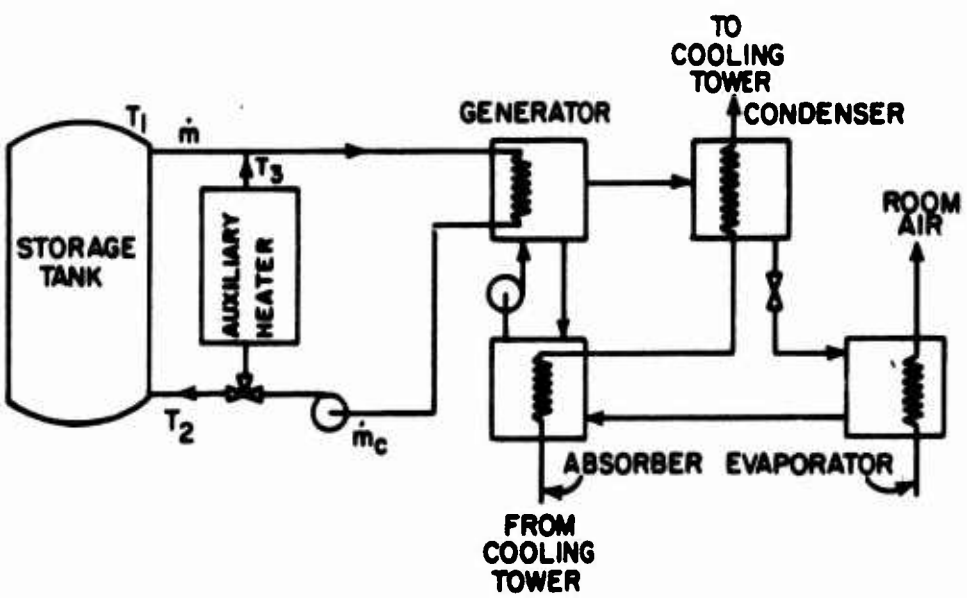

Figure C8. Solar-powered air-conditioning system schematic.

The values of the outputs are

$$\dot{m} = Y\dot{m}_c, \; T_2 = T_1 - \frac{(q_s)_{max}}{\dot{m}_c c_p COP},$$

$$Q_s = Y(q_s)_{max}/COP, \text{ and } Q_a = \frac{(1-Y)(q_s)_{max}}{COP}.$$

Finally, there may be no cooling load. It is also assumed that there is no energy demand when there is a cooling load, but that the outside temperature is below some specified value, e.g., 60°F (15.5°C). Then, either the cooling system will include means of introducing outside air, or the building occupants will open windows.

Storage Tank Equations

Energy is stored as sensible heat in fluid in the storage tank and is lost from the storage tanks to its surroundings. The loss coefficient, U, is a parameter which must be calculated for the type and amount of tank insulation. The model assumes a constant value for the temperature of the surrounding environment. (While this would be a good assumption for a tank inside the house, it is probably not a good assumption for the tank buried outside the house; no better model was readily available, however.) Only one card would have to be changed for the energy loss from the tank to be subtracted from the heating load or added to the cooling load.

It is possible that the temperature at which energy is collected will exceed the boiling temperature of the storage fluid. The model assumes that boiling may occur, with energy being dissipated through a pressure relief valve. The boiling temperature is a system parameter.

The energy stored in the tank is given by $E = mc_pT$, with $T = 0$ defining the zero energy level. The rate of tank energy change is the sum of the energy rates produced or consumed by the other components.

Rate of energy gain from collector

$$q_c = \dot{m}_c c_p (T_c - T_t)$$

Rate of energy loss to heater

$$q_h = \dot{m}_h c_p (T_t - T_h)$$

Rate of energy loss to air conditioner

$$q_a = \dot{m}_a c_p (T_t - T_a)$$

Rate of energy loss to environment

$$q_l = UA (T_t - T_e)$$

where $\dot{m}_c$, $\dot{m}_h$, and $\dot{m}_a$ are the average flow rates to the components, and T_c, T_h, and T_a are the return temperatures. T_t is the average tank temperature, and A is the tank surface area, yielding

$$\frac{dE}{dt} = F = q_c - q_h - q_a - q_l \qquad \text{(Eq C18)}$$

The safety relief compares the tank's total energy to the maximum energy permitted by the boiling point limit.

$$E_{max} = mc_p T_{boil}$$

$$E = E_o + F\Delta t$$

Energy lost by boiling in the tank is

$$q_{over} = E - E_{max} \text{ if } E > E_{max}$$

$$q_{over} = 0 \qquad \text{if } E \leq E_{max}$$

This gives a revised rate of change of tank energy,

$$F = F - \frac{q_{over}}{\Delta t} \qquad \text{(Eq C19)}$$

REFERENCES

ASHRAE Handbook of Fundamentals (American Society of Heating, Refrigerating, and Air Conditioning Engineers, Inc., 1972).

Bliss, R. W., "The Derivation of Several Plate Efficiency Factors Useful in the Design of Flat-Plate Solar Heat Collectors," *Solar Energy*, Vol 3, No. 4 (1959).

Butz, L. W., et al., *Use of Solar Energy for Residential Heating and Cooling*, M.S. Thesis in Mechanical Engineering (University of Wisconsin, 1973).

Catalog on Solar Energy Heating and Cooling Products (Energy Research and Development Administration, 1975).

Climatic Atlas of the United States (U.S. Department of Commerce, 1968).

Correspondence from Dr. Philip Anderson, Arkansas-Louisiana Gas Company (ARKLA) to Doug Hittle (CERL); subject: ARKLA cooler, February 27, 1974.

Duffie, J. A. and W. A. Beckman, *Solar Energy Thermal Processes* (John Wiley and Sons, 1974).

FORTRAN Extended, Version 4, Reference Manual (Control Data Corporation, 1974).

Hill, J. S. and T. Kusuda, *Methods of Testing for Rating Solar Collectors Based on Thermal Performance*, NBSIR-74-635 (Thermal Engineering Systems Section, Center for Building Technology, National Bureau of Standards, December 1974).

Interim Performance Criteria for Solar Heating and Cooling Systems and Dwellings (National Bureau of Standards, January 1, 1975).

Kelly, G. E. and J. E. Hill, *Method of Testing for Rating Thermal Storage Devices Based on Thermal Performance*, NBSIR-74-634 (Thermal Engineering Section, Center for Building Technology, National Bureau of Standards, May 1975).

Klein, S. A., "Calculation of Flat-Plate Collector Loss Coefficients," paper presented at U. S Section meeting, International Solar Energy Society, Fort Collins, CO (1974).

NBSLD, Computer Program for Heating and Cooling Loads in Buildings (National Bureau of Standards, 1974).

OCE Life Cycle Costing Instructions (Department of the Army, May 1971).

CERL DISTRIBUTION

Chief of Engineers
ATTN: DAEN-MCZ-S (2)
ATTN: DAEN-MCE (5)
ATTN: DAEN-ASI-L
ATTN: DAEN-FEE-A
ATTN: DAEN-FE
ATTN: DAEN-RD
ATTN: DAEN-CWZ-R (3)
ATTN: DAEN-CWR-R (2)
ATTN: DAEN-ZCI
Dept of the Army
WASH DC 20314

U.S. Military Academy
ATTN: Dept of Mechanics
ATTN: Library
West Point, NY 10996

The Engineering School
Technical Information Br.
Archives Section (Bldg 270)
Ft Belvoir, VA 22060

USA Engineering School
ATTN: ATSEN-DT-LD (2)
Ft Belvoir, VA 22060

Director
USA Cold Regions Research
Engineering Laboratory
PO Box 282
Hanover, NH 03755

Director, USA-WES
ATTN: Library
PO Box 631
Vicksburg, MS 39181

Deputy Chief of Staff
for Logistics
US Army, The Pentagon
WASH DC 20310

The Army Library
Office of the Adjutant
General
Room 1A530, The Pentagon
WASH DC 20315

HQDA (SGRD/Chief),
Sanitary Engr Br
WASH DC 20314

Dept of the Army
ATTN: EACICT-P
HQ I Corps (Group)
APO San Francisco 96358

Commander-in-Chief
US Army, Europe
ATTN: AEAN
APO New York, NY 09403

Commander, Naval Facilities
Engineering Command
ATTN: Dep Ass't Commander
for Design & Spec (04D)
ATTN: Code 04
200 Stovall Street
Alexandria, VA 22332

Chief, Naval Operations
ATTN: The Library
Dept of the Navy
WASH DC 20360

Naval Civil Engineering Lab
Technical Library Code L31
Port Hueneme, CA 93043

Officer in Charge
Naval Civil Engineering Lab
Port Hueneme, CA 93043

AF Civil Engr Center/PG
Tyndall AFB, FL 32401

Air Force Weapons Lab
ATTN: Civil Engr Div
ATTN: Technical Library (DOUL)
ATTN: AFWL/DE
Kirtland AFB, NM 87117

AF/PREE
Bolling AFB, DC 20332

AD/RDPQ
WASH DC 20330

Each Division Engineer
US Army Engr Div
ATTN: Library
ATTN: Chief, Engr Div

Each District Engineer
US Army Engr District
ATTN: Library
ATTN: Chief, Engr Div

Defense Documentation Center
ATTN: TCA (12)
Cameron Station
Alexandria, VA 22314

Engineering Societies Library
345 East 47th Street
New York, NY 10017

Library of Congress (2)
Exchange and Gift Div
ATTN: American & British
WASH DC 20540

Superintendent of Documents
Div of Public Documents
ATTN: Library (2)
US Govt Printing Office
WASH DC 20402

Engineer
US Army, Alaska
APO Seattle, WA 98749

Commander, TRADOC
Office of the Engineer
ATTN: ATEN
Ft Monroe, VA 23651

Bldg Research Advisory Board
National Academy of Sciences
2101 Constitution Avenue
WASH DC 20418

Commanding General
US Army Forces Command
ATTN: AFEN-FEB
Ft McPherson, GA 30330

Commanding General, 5th USA
ATTN: Engineer
Ft Sam Houston, TX 78234

Commanding General, 6th USA
ATTN: Engineer
Presidio of San Francisco, CA
94129

Institute of Defense Analysis
400 Army-Navy Drive
Arlington, VA 22202

Defense Logistics Studies Information Exchange (2)
U.S. Army Logistics Management Center
ATTN: AMXMC-D
Ft Lee, VA 23801

Coastal Engineering Research Center
Kingman Bldg
ATTN: Library
Ft Belvoir, VA 22060

Dept of the Army
HQ 15th Engineer Battalion
9th Infantry Division
Ft Lewis, WA 98433

Dept of the Army
U.S. Army Human Engr Lab
ATTN: AMZHE/J. D. Weisz
Aberdeen Proving Ground, MD 21005

314/DEEE
Little Rock Air Force Base
Jacksonville, AR 72076

Commander
U.S. Army Foreign Science and Technology Center
220 7th St, NE
Charlottesville, VA 22901

Commander
U.S. Army Science and Technology Information Team - Europe
APO New York, 00710

Commander
U.S. Army Science and Technology
Center - Far East Office
APO San Francisco 96238

Los Alamos Scientific Laboratory
ATTN: Bruce Hunn/Mail Stop 985
Los Alamos, NM 87545

Army Air Force Exchange
Service
ATTN: EN-C/George Williams
Dallas, TX 75222

Mr. Kuharick (Phoenix House)
P.O. Box 7246
Colorado Springs, CO 80933

Sherril Glover
Sverdrup Parcel
St Louis, MO

U.S. Naval Civil Engr Lab
ATTN: Ralph J. Tinsley, Solar R&D
Port Hueneme, CA 93043

Bill Carson, Master Planner
ATTN: AMXSH - SFS
Lathrop, CA 95330

Energy Resources Center
ATTN: J. H. Armstead, Jr.
University of Illinois,
Circle Campus
Chicago, IL 60680

Energy Management Consultants,
Inc.
ATTN: Don E. Croy
7456 West 5th Avenue
Denver, CO 80226

Each Major Facility Engr